sUAS sensor selection and utilization for remotely sensing crop health and production parameters

by

Harman Singh Sangha

B.Tech., Punjab Agricultural University, 2015

A THESIS

Submitted in partial fulfillment of the requirements for the degree

MASTER OF SCIENCE

Department of Biological and Agricultural Engineering
Carl R. Ice College of Engineering

KANSAS STATE UNIVERSITY
Manhattan, Kansas

2019

Approved by:

Major Professor
Dr. Ajay Sharda

Copyright

Abstract

Since the beginning of 21st century technological innovations are aiding to improve the agricultural industry. Precision Agriculture (PA) systems are one of those technologies which are creating the greatest impact on agricultural practices. PA is defined as the farming practices which optimizes the farm inputs with a goal to increase overall yield and minimizing harmful environmental impacts. To accomplish such targets, collection of high resolution spatial and temporal data on crop health and physiology becomes critical in helping to make decisions on optimizing farm inputs. Due to this, there has been increase in the use of small unmanned aerial systems (sUAS) in agricultural industry as a PA tool. sUAS are used for remote sensing applications such as crop phenotyping, crop water stress estimation, crop disease detection among others. With the development of robust sUAS sensors, collection of vegetative based data in field is evolving into standalone system. Sensors chosen for such applications include RGB sensors, thermal infrared sensors, modified color infrared sensors, multispectral sensors and Hyperspectral sensors. Usually a sUAS sensor is selected based on the spectral ability of the sensor and specific configuration are not considered. Improper selection of sensors leads to false data collection affecting the studies done using these sensors.

In this thesis thermal infrared, modified color infrared and multispectral sensors were identified and compared based on the parameters specific to the sensor involved, to understand and improve future selection of sUAS sensors.

Multispectral sensors are more commonly used as compared to other UAS sensors as multispectral sensors provide information both in visible and infrared spectrum. Multispectral sensors can be divided into two categories, namely narrowband and broadband. A study was done to compare and evaluate performance of the two types of multispectral sensors available in precision agriculture systems. The sensors were examined on different parameters to check their ability to provide remote sensing data with high-accuracy. Spectral response, ground resolution and statistical correlation with ground data were evaluated for both the sensors. Results shows the sensors performed differently in different parameters, but the spectral data provided by them was in close correlation with each other. A need for developing better ground data collection methods was observed.

Thermal image quality is critical to accurately quantify water stress patterns in field crops. Image data quality from a thermal sensor is impacted by several factor. A second experiment was conducted with goal to compare accuracy of canopy temperature quantification and assess the quality of thermal orthomosaic when using thermal sensor of different focal length and image acquisition at varying flying altitudes of a sUAS. Three thermal infrared cameras were selected with focal lengths of 9mm, 13mm, and 19mm. All three cameras were flown at altitudes of 20m, 50m, and 80m. Results showed that 13 mm focal length and 50 m altitude produce finer resolution orthomosaic which provide a robust and accurate information on canopy temperature. Overall, the canopy temperatures were quantified accurately regardless of altitude and focal length by efficiently and accurately utilizing the ground reference system.

Table of Contents

List of Figures

List of Tables

Acknowledgements

My research would not have been possible without the help and support of Dr. Ajay Sharda, my advisor. Dr. Sharda provided invaluable insight and guidance throughout the duration of my project. His dedication of time, resources, and knowledge provided allowed me to grow personally and professionally. I would also like to thank my committee members: Dr. William Schapaugh Jr. and Dr. Deon van der Merwe. Both provided physical resources and countless hours of knowledge and guidance through the duration of my project. I have thoroughly enjoyed the opportunity to work with both of them.

Preface

All work presented in this thesis was conducted at Kansas State University in Manhattan, KS in the Biological and Agricultural Engineering Department. The following thesis chapters were written for direct submission for individual publication.

Chapter 1 - Introduction

Due to the ever increasing population, crop production must increase approximately 25-70 % from rcurrent levels to meet future demands (Hunter et al., 2017). To reach higher efficiencies, the environment is often ignored. Sustainable agriculture helps to avoid unwanted degradation of the agricultural lands along with increasing the farm yields. Precision agriculture is a farming practice in which farm inputs are optimized, overall efficiency of the farm is improved, and environmental footprint is reduced by concentrating on right management practice at right place at right time and at right rate (Gebbers and Adamchuk, 2010; Khanal et al., 2017; Hunt and Daughtry, 2018). Remote sensing is a important part of precision agriculture (Robert, 1982; Mulla and Khosla, 2016; Moran, Inoue and Barnes, 1997; Brisco et al., 1998).

Designed initially for military purposes, unmanned aerial systems (UAS) are now increasingly used in agricultural fields as remote sensing platforms (Joshua, 2017). UAS provide an alternate solution to traditionally used satellite and aircraft remote sensing. UAS are more flexible to use and economically affordable compared to other remote sensing platforms (Zhang and Kovacs, 2012). UAS are successfully been used for remote sensing applications such as vegetation index calculations, species phenotyping, water stress identification, etc. (Berni et al., 2009; Baluja et al., 2012; Zaman-Allah et al., 2015; Senthilnath et al., 2017).

There are a variety of sUAS sensors are used onboard, but the most frequently used in agriculture are the standard Red-Green-Blue camera, multispectral, hyperspectral and thermal sensors. The type of information collected through remote sensing is decided by the sensor used which influences the nature of the application. A digital camera senses only visible light from the red, blue, and green wavelengths, and the combined RGB bands are used to produce the typical color image. Multispectral sensors deliver additional information by sensing data from non-visible

wavelengths as well as visible. Hyperspectral sensors collect data on hundreds of narrow, contiguous spectral bands which can provide specific information on particular wavelengths (Joshua, 2017). Thermal sensors are capable of capturing just the long wave infrared which helps in identifying water stress in field crops.

Availability of a variety of sensors and platforms is better for research purposes, however, it is critical to choose the correct sensor for the application. Before selecting a sensor, researchers consider data outputs from the sensor. Common concerns that arise are whether the spatial resolution is adequate to provide accurate and robust data for analytics and whether the images can be efficiently stitched to generate geometrically accurate orthomosaics. A sensor is often selected based on the ability of the sensor to detect certain wavelengths and specific configuration such as focal length, sensors size, bandwidth and radiometric resolution are not considered.

Considering the stated issue regarding camera selection for remote sensing purposes on UAS, this study was designed to compare and evaluate performance of the types of inrared sensors commonly used in precision agriculture with the following objectives:

- Compare and contrast the differences between PI extracted from both narrowband and broadband multispectral sensors.
- Check correlations between extracted data from remotely sensed imagery with ground data collected during the growing season.
- Assess relative merits of PI derived from broadband and narrowband sensors to assess crop growth parameters.
- Develop crop canopy thermal orthomosaic from aerial imagery collected at varying altitudes using thermal sensors of different focal lengths
- Conduct qualitative and quantitative analysis on different images and thermal orthomosaics.

Chapter 2 - Infrared remote sensing using unmanned aerial vehicles for evaluating crop health parameter: A review

Abstract

Global food demand is increasing due to this it is crucial to make farm operations more efficient and to reduce agricultural losses. Measuring spatial variability within the crop field is crucial to achieve this objective. Precision agriculture make use of various technologies such as remote sensing, sensors, global positioning system to provide in-field information which makes local management of agricultural inputs feasible. Remote sensing being one of the most important tool contributes by helping researchers to estimate in-filed variations. Platforms involved for remote sensing are satellites, aircrafts, unmanned aerial systems and ground sensors. Compared to satellites and aircrafts, unmanned aerial systems are flexible to use and are economic. Number of sensors are used onboard unmanned aerial systems. They include standard visible cameras, multispectral cameras, hyperspectral cameras and thermal cameras. Sensors are selected based upon the information which is required regarding the crop canopy. This paper reviews the applications of sensors used on unmanned aerial systems for evaluating crop health parameters.

Introduction

The world's population is expected to grow to 9 billion by 2044 (Bureau, 2011). Due to this there is going to be an increasing global food demands to meet the population needs. With the increasing global demand in food and agricultural outputs it becomes important to reduce agricultural losses and make farming operations more efficient (Crimmins 2016). For reducing environmental impact and optimizing the use of agricultural inputs, measuring spatial variability in above and below ground becomes a crucial task. The techniques which are used to measure

agricultural entities and help apply appropriate corrections is known as Precision Agriculture (PA) (Khanal, 2017). Precision agriculture apply a combination of technologies such as the Global Positioning System (GPS), remote sensing (RS), electronic sensors and devices, geographic information system (GIS) in order to provide the necessary information to make feasible the local management of the agricultural activities at within-field detail (Khanal, 2017).

Remote sensing is the most commonly used tool in precision agriculture. RS plays a crucial role in serving researchers to estimate in-field variations (Joshua, 2017). This is done by measuring reflectance or emittance of electromagnetic waves which are produced by the plants after interacting with sunlight. Properties about a crop can be known by observing the reflectance or emittance values for the different wavelengths of light (Arthur et al., 2015). Remote sensing platforms include ground sensors, satellites, aircrafts and small unmanned aerial system (sUAS) sensors. The development of UAV in the last decade has led to a new era in remote sensing, providing data of high spatial, spectral, and temporal resolution (Colomina, 2014). UAS provide an alternate option to traditionally used satellite and aircraft to collect data as they are more independent from climatic variables, they are flexible to use and are economic as compared to other remote sensing platforms (Zhang and Kovacs, 2012).

There are a variety of sUAS sensors accessible to the user, but the most frequently used in agriculture are the standard RGB (Red-Green-Blue) camera, multispectral, hyperspectral and thermal sensors. The quantity and quality of information collected through remote sensing is decided by the type of sensor used which influences the nature of the application. A digital camera senses only visible light from the red, blue, and green wavelengths, and the combined RGB bands are used to produce the typical color image. Multispectral sensors deliver additional information by sensing data from non-visible wavelengths as well as visible. Hyperspectral sensors collect data

on hundreds of narrow, contiguous spectral bands which can provide specific information on particular wavelengths (Joshua, 2017). Thermal sensors are capable of capturing just the long wave infrared which helps in identifying water stress in field crops.

The objective of this chapter is to review the use of infrared remote sensing using unmanned aerial vehicles for evaluating crop health and production parameters. We'll discuss the kinds of sUAS platforms which are used for remote sensing applications. Sensors types will be discussed in brief. And finally we'll look various application of these sensors in agricultural fields such as disease detection, drought stress detection, yield estimation, pigment concentration, etc.

sUAS platforms

Originally made for military purposes, sUAS has witnessed an increase in their usage over the last decade as a remote sensing platform for agricultural applications (Joshua, 2017). A variety of sUAS platforms have been developed over the years. There are two main types of sUAS which are majorly used in agricultural applications: rotary-motor and fixed-wing. Fixed-wing airplane designs were studied by Beard et al., 2005and Everaerts, 2008, where they developed their own autopilots to be used on sUAS. Rotary-wing systems were developed and tested by Ehsani, Sankaran, Maja, & Neto, 2014 and Lucieer, Malenovský, Veness, & Wallace, 2014 for to be used in horticulture and seasonal crop sensing. Each aircraft type has its own benefits and drawbacks. Rotary-motor systems is known to have a longer lifecycle since they are able to do vertical takeoff and landing, and their flights are more stable. Conversely, their flight speeds are slower and they are not capable of covering much area due to limitations on their battery life. Fixed-wing systems are able to cover more area per flight but are comparatively expensive and have the affinity to breakdown after multiple crash landings, which is the usual landing style for a fixed wing system. However, fixed wings can take-off with a larger payload than the rotary style platforms (Shi et al.,

2016). sUAS have shown great promise as tools for agricultural and environmental applications in recent years (Lucieer et al., 2014). The cost of collecting data using a UAS is less than using satellite data, but the cost for data processing rises considerably as the size of the area of interest increases (Matese et al., 2015).

sUAS camera sensors

Different types of camera sensors are being used for remote sensing purposes. The selection of a camera is based on application, dimensional size, focal length, wavelengths observed, etc. The sensor types can be RGB true color, thermal infrared (TIR), multispectral broadband camera (MSB), multispectral camera, hyperspectral camera and other sensors (Majidi and Bab-Hadiashar, 2005; Berni et al, 2009; Zarco-Tejada et al., 2005; Kingston and Beard, 2004). RGB (red-green-blue) cameras are cheap and have high spatial resolution (Nijland, 2014). Not many vegetative indices can be calculated using RGB cameras but they can be used to generate digital elevation models and vegetative height maps (Maes, 2019). Secondly there are multispectral cameras, they are made to sense the near-infrared (NIR) spectrum alongside with the visible RGB spectrum. Multispectral cameras can be of two types, modified RGB and narrowband multispectral. Modified RGB cameras are the one which have their NIR filter replaced with a red filter, this makes the earlier red band sensitive to NIR spectrum (Berra, 2017).Even though they have only 3 observable bands, the bandwidth for a single band in modified RGB cameras usually ranges between 100-110 nm. Narrowband multispectral cameras have more spectral resolution, it consists a set of sensors with each sensor measuring in one spectral region (Maes, 2019). In narrowband multispectral cameras the sensing elements have a working bandwidth of between 10-40 nm. Due to this difference between modified RGB and narrowband multispectral cameras, they are used to very specific application depending upon what information is required from the sensor.

The third type of UAV sensors are Hyperspectral cameras. They cover the spectrum for electromagnetic radiation related to crop health and monitoring (~ 400-1000 nm) in narrow bands usually <10 nm. They can have up to 250 different bands based on the product which is being used. Hyperspectral cameras don't have much application right now but their use is predicted to increase in coming years (Adao, 2017). Lastly thermal cameras are low resolution cameras with only one band measured using a microbolometer sensor sensitive to longwave infrared region (7000-13000 nm). They have a common sensor size of 640x512 pixels, which is small as compared to multispectral and hyperspectral sensors which are used in remote sensing applications. Thermal sensors are typically used to extract canopy temperature or to create crop water stress maps.

Remote sensing applications

In the following sub-sections we discuss some of the major applications of remote sensing using sUAS in assessing crop health and physiology.

Crop phenotyping

Yang et al. 2017, has reviewed various crop phenotyping application of remote sensing using sUAS. The sUAS are mounted with different camera sensors to quickly and non-invasively collect high-resolution imagery data of the crop fields. After this various crop models are used to extract information from the imagery after the images were processed and stitched together (Sugiura et al., 2005; Li W. et al., 2016). sUAS have been successfully demonstrated their usefulness in obtaining crop geometric traits like vegetative cover (Weiss and Baret, 2017; Yu et al., 2017), crop height (Bareth et al., 2016; Holman et al., 2016), lodging (Chapman et al., 2014), canopy structure (Aasen et al., 2015; Weiss and Baret, 2017), leaf area index (Carcoles et al., 2013) and emergence (Sankaran et al., 2015) by processing and analyzing imagery collected by onboard camera sensors (Tamouridou et al., 2017; Yu et al., 2017). Crop identification and leaf color

monitoring is possible with image feature analysis using remote sensing image classification (Geipel et al., 2014). Canopy cover is considered an important factor while observing crop transpiration and photosynthesis (Mullan and Reynolds, 2010). Crop canopy dynamics over time is recognized as one of the important phenotyping traits in crop breeding (Zaman-Allah et al., 2015; Yu et al., 2017). Surface temperature and crop reflectance can be used to approximate crop canopy cover (Booth et al., 2005; Rajan and Maas, 2009).

Disease detection

Often crop and plantations are affected by diseases which results in product and capital losses, sometimes up to billions of dollars nationwide. Farmers are the one hugely affected by disease infestation in their crops. For minimizing losses and increasing yield, instantaneous detection of diseases is required. Multispectral imagery have been used and demonstrated as a tool to assess disease symptoms and severity. Infrared and visible spectroscopy (S. Sankaran et al., 2010) and multispectral imagery (Garcia-Ruiz et al., 2013; Yang et al., 2010) can be used to early detect diseases in crops. Certain diseases can be identified by observing specific bands in the infrared region which provide information on the crop stress levels. Specific wavelengths are reflected by different plants which can be used to assess severity and the type of disease on the affected crop (S. Sankaran et al., 2010). Green normalized difference vegetative index (GNDVI) and soil-adjusted vegetative index (SAI) can be used to assess huanglongbing infestation in citrus trees (Garcia-Ruiz et al., 2013). Sudden death syndrome (SDS) in soybeans was found to be strongly correlated to pigment index (PI) collected using multispectral imagery (Hatton, 2018).

Drought stress detection

Drought conditions are often experienced in crop fields which are rain fed. Also in irrigated field crops can experience water stress if irrigation is not applied in time. One of the biggest

challenges in agriculture is proficient use of water resources with the help of precision irrigation systems (Rockström et al., 2017; Ding, 2018). Thermal imagery is highly suitable for early detection of water stress, as crop canopy temperature decreases when the plant is transpiring and the canopy temperature increases when the plant is not transpiring due to lack of water availability (Maes and Steppe, 2012; Gago et al., 2015). Some sUAS studies were able to extract stomatal conductance from crop canopy data (Berni et al., 2009; Gago et al., 2017). Crop water stress index (CWSI) is also commonly used by researchers to detect water stress by normalizing crop canopy temperature data. Fresh methods are being studied to study crop water stress where narrow-band VI are created using hyperspectral imagery. A normalized form of photochemical reflectance index has been proposed as a water stress detection tool (Zarco-Tajeda et al., 2013).

Weed detection

Infestation of weeds in agricultural crops is observed quite often. It is usually patchy and difficult to find within the crop which makes it time consuming to take required measures. sUAS provide a better way to identify and map the weeds within the crop. Site-specific weed management is a term which is often used with sUAS based weed control methods. Many studies have shown the use of sUAS imagery to develop site-specific weed management systems. Spectral responses of different weeds are different as compared to that of crops, which means supervised classification methods can be used successfully using modified RGB cameras (Alexandridis, T. et al., 2017; Tamouridou, A.A. et al., 2017). Supervised learning is a time-consuming method and better outcomes cannot be always guaranteed (Lambert, J. et al., 2018). Machine learning methods which are trained on ground-based data set are faster alternates to supervised learning (Chlingaryan, A. et al., 2018). Object-based image analysis is another method which is used in differentiating weeds from crops. In this method group of pixels with comparable spectral response

are used for analysis as compared to analyzing individual pixel. Significant decrease in herbicide use was observed when prescription maps were made using this technology (de Castro, A.I. et al., 2018; López-Granados, F. et al., 2016a; López-Granados, F. et al., 2016b).

Estimating chlorophyll concentration

The process of photosynthesis is used by the plants to produce chemical energy from solar energy. Chlorophyll concentration is vital to photosynthetic process as they are one of the primary pigment used for photosynthesis. Use of multispectral imagery to estimate chlorophyll content has been successfully demonstrated by few studies. Swain et al., 2007 and Tilling et al., 2007 showed that chlorophyll can be directly measured using canopy chlorophyll index. Hunt Jr. et al 2013 used triangular greenness index as a method to estimate chlorophyll content.

Calculating biomass

For better crop management and effective crop growth monitoring, information regarding in-field variation of crop growth and biomass is extremely useful to farmers. Studies have shown that vegetative indices derived from RGB imagery can be used to check up on growth stages of cereal crops quite successfully (Schirrmann, M. et al., 2016; Du, M.M. and Noguchi, N., 2017; Burkart, A. et al., 2018). Crop height calculated from digital elevation models which are made using RGB imagery from sUAS are a good estimator of actual height (Madec, S. et al., 2017; Watanabe, K. et al., 2017; Hu, P.C. et al., 2018; Brocks, S. and Bareth, G., 2018; Diaz-Varela, R.A. et al., 2015; Dillen, M. et al., 2016). Vegetative indices can be combined with crop height data to obtain in-field biomass estimates (Bendig, J. et al., 2015; Yue, J.B. et al., 2017). Also several studies used the same method to map lodging in crop fields (Du, M.M. and Noguchi, N., 2017; Wang, J.-J. et al., 2018; Chu, T.X. et al., 2017; Yang, M.-D. et al., 2017). Another study

used a separate approach by combining RGB and thermal imagery to improve the efficiency of assessing lodging (Liu, T. et al., 2018).

Predicting yield

Accurate prediction of yield is of quite importance to both the farmer and agricultural industry. Vegetative indices and plant height calculated using RGB imagery and multispectral imagery has been used successfully to estimate crop yields (Chu, T. et al., 2016; Du, M.M. and Noguchi, N., 2017; Gracia-Romero, A. et al., 2017; Kyratzis, A.C. et al., 2017; Zhou, X. et al., 2017). Regression models have been focused on so far for all the studies done on estimating yields. These models usually cannot be applied to crop on the same location for consecutive year or at different location for the same year but can be scaled up to entire field for same location and same year (Rembold, F. et al., 2013).

Conclusion

Remote sensing applications using sUAS in agricultural industry are growing day by day. The various aircrafts being used for such applications were reviewed. Also different sensors which are used onboard sUAS for collecting spectral data were studied. Finally, specific agricultural applications of remote sensing were examined such as crop phenotyping, disease detection, drought stress detection among others. It was observed that all kind of spectral sensors can be used onboard sUAS with great efficiency. But it was noticed that the sensors used in these studies were the one which were already available with the researcher or which are easily available commercially. Consideration was not given to examine and compare specifications related to each sensor, such as sensor size and radiometric resolution. Also other sUAS parameters such as flying altitude and flight speed were not properly evaluated. There is a need to understand these parameters to expand the knowledge which is available regarding sUAS and sensors used onboard

them. This information can improve the quality of data collected on crops using sUAS sensors. Having this idea in consideration, in this thesis thermal infrared, modified color infrared and multispectral sensors were identified and compared based on the parameters specific to the sensor involved, to understand and improve future selection of sUAS sensors.

Chapter 3 - Comparison of multispectral platforms for calculating pigment index by referencing ground data

Abstract

Vegetative based data collection is evolving due to development of more robust and lightweight sensors. Among these sensors, multispectral sensors are popular among researchers owing to their wide range of application. There are two kinds of multispectral sensors, narrowband and broadband sensors. A multispectral sensor is selected as per according its ability analyze specific wavelengths and sensor configuration such as focal length, sensor size and radiometric resolution are not given consideration. Therefore, this study was conducted to compare multispectral sensors for calculating pigment index by referencing ground data. A narrowband and broadband sensor was flown over soybean field using a quadcopter. Imagery data was compared for ground resolution, orthomosaic quality and statistical comparison with ground data. Broadband sensor performed better in capturing detailed spatial information. Broadband sensor was found to be highly correlated soybean maturity ($r = 0.83$, $p \leq 0.001$). Ground data collected was of coarse resolution as compared to spectral data. Better resolution ground data can confirm spectral responses as crop parameter. Narrowband sensor was limited in its ability to calculate pigment index. In future, other indicies will be examined which can be calculated from multispectral sensors to compare with ground data.

Introduction

There is a lot of pressure on current agricultural fields to produce food for the ever growing human population (Hunter et al., 2017). In the effort to reach this goal, the environment is often ignored to reach higher efficiencies. The concept of sustainable agriculture has been introduced to

avoid unwanted degradation of the agricultural lands. A sustainable system should be resource conserving, socially supportive, commercially competitive and environmentally sound (Ikerd, 1990). Precision agriculture (PA) is a major contributing factor in helping us to create a more sustainable agriculture environment. PA has a goal to optimize use of resources to increase sustainability and profitability of agricultural systems by keeping environmental impact at a minimum and improve the quality of social aspects of agriculture (Gebbers and Adamchuk, 2010). PA provides tools and technologies to identify in-fields soil and crop variability, offering a means to improve sub-field level farming practices and optimizing agronomic inputs (Khanal, 2017).

Remote sensing plays a central role in attaining that goal by helping researchers determine in-field variation. This can be done by measuring reflectance or emittance of electromagnetic waves which are produced by the plants after interacting with sunlight. Properties about a crop can be determined by observing the reflectance or emittance values for the different wavelengths of light (Arthur et al., 2015). Designed primarily for military applications, unmanned aerial systems (UAS) are now being increasingly used in agricultural scenarios as remote sensing platforms (Joshua, 2017). UAS provide an alternate option to traditionally used satellite and aircraft to collect data as they are more independent from climatic variables, they are flexible to use and are economical compared to other remote sensing platforms (Zhang and Kovacs, 2012). Also the data can be obtained in higher resolution which could provide critical information for phenotyping studies on crops, disease detection and crop stress evaluation (Berni et al., 2009; Baluja et al., 2012; Candiago et al., 2015; Zaman-Allah et al., 2015; Senthilnath et al., 2017).

With the development of robust and lightweight sensors, collecting vegetative based data in field is rapidly evolving into standalone systems (Berni et al., 2009). The use of UAS based sensors to detect water stress and to quantify biomass in crops has been successfully demonstrated

by many researchers (Bendig et al., 2015; Park et. al., 2015). The kind of information collected using remote sensing depends on the type of sensor used and sensor selection is based on the application in which it will be used. The sensors types can be classified broadly as Red-Green-Blue (RGB) sensors, thermal infrared (TIR) sensors, modified color infrared (CIR), narrowband multispectral sensor and hyperspectral sensors (Kingston and Beard, 2004; Majidi and Bab-Hadiashar, 2005; Zarco-Tejada et al., 2005; Berni et al, 2009).

Multispectral sensors are more commonly used by farmers and researchers compared to other UAS sensors since multispectral sensors provide information both in the visible and infrared spectrums (Joshua, 2017). Multispectral sensors can be divided into two categories, namely narrowband and broadband. A typical narrowband multispectral sensor has a bandwidth of 10 nm whereas broadband sensors have a bandwidth ranging from 40 nm to 110 nm (Lei deng, 2018). Both type of sensors can be used for estimating crop variables, but it is often found that information extracted from narrowband and broadband sensors when compared with each other are neither in complete agreement nor conflict (Zhao, 2007). Usually a multispectral sensor is selected based on the ability of the sensor to detect certain wavelengths and specific configuration such as focal length, sensors size, bandwidth and radiometric resolution are not considered.

Considering the stated issue regarding camera selection for remote sensing purposes on UAS, this study was designed to compare and evaluate performance of the two types of multispectral sensors commonly used in precision agriculture. The sensors were examined to assess differences in their ability to provide accurate remotely sensed data and derive a Pigment Index (PI) for multiple flights in the season. In this study the following objectives were set:

- Compare and contrast the differences between PI extracted from both narrowband and broadband multispectral sensors.

- Check correlations between extracted data from remotely sensed imagery with ground data collected during the growing season.
- Assess relative merits of PI derived from broadband and narrowband sensors to assess crop growth parameters.

Methods

sUAS and cameras

A Matrice – 100 (DJI, Shenzhen, China) quadcopter was used to perform the aerial missions (Fig. 3.1). The quadcopter could handle a maximum payload of 1 kilogram. The UAS was equipped with in-built autopilot and custom missions can be uploaded on the copter using third party applications. It has dual battery compatibility each battery providing 5700mAh power to the copter, providing 25 minutes of effective flight time with multispectral sensors (185-350 gm) onboard. The quadcopter can fly in wind speeds of up to 10 m/s but to maintain safety standards and to avoid error in data caused due to wind influence data was collected when the wind speeds were less than 4.5 m/s. The sensors were mounted using a custom made 3-D printed gimbal. The copter was used to collect color infrared imagery to compare multispectral cameras.

Figure 3.1. Matrice 100 quadcopter which was used for collecting infrared data

Two kinds of multispectral sensors, one was a narrowband sensor Micasense Rededge-M (Micasense Inc., Seattle, WA) with 5 bands of blue, green, red, red-edge and near infrared. The bandwidth varied from 10 nm to 40 nm for this sensor with 1.2 MP of sensor size. The second sensor was a modified broadband infrared Sony α5100 (Sony corporation of America, New York, NY). It had 3 bands of blue, green and near infrared. Modified broadband cameras have broader bands as compared to Micasense sensor close to 100 nm with 24 MP of sensor size. The Micasense sensor had a global shutter whereas Sony α5100 had a rolling shutter. Also, a Flir Vue pro R 13 mm (Flir Systems Inc, Wilsonville, OR, USA) thermal infrared camera was used to collect thermal aerial imagery in °C and cross verify spectral response from both multispectral cameras (Fig. 3.2).

Figure 3.2. Camera sensor used for this study: a) Micasense Rededge-M b) Flir Vue pro R 13 mm c) Sony α5100 modified CIR

Crops and Missions

The crop selected for this study was soybean (Fig. 3.3a). The plot was located south of Assaria, KS (38.669030° N, -97.604247° W). The agronomic performance Roundup Ready 2 Xtend® commercial soybean cultivars was evaluated under dryland conditions as part of the Kansas Soybean Variety Performance Test Trials. Each cultivar was planted in 4-row plots, 3.7 m long, spaced .76 m apart. The experimental design was a randomized complete block with 4 replications. Planting rate was 30 seeds per m of row. The soil type at the site was a Detroit silty clay loam. There were total 35 cultivars represented as E1, E2, etc. The missions were created on

Mission Planner (Mission Planner®, by Michel Oborne) autopilot software suite. Mission Planner was used as a configuration utility and as a dynamic control supplement for compatible autonomous vehicles. After determining the mission characteristics, the mission files were imported into a third party autonomous flight application (Litchi® for DJI). Litchi allowed mission files from Mission Planner to be uploaded onto the quadcopter. This function is not available within DJI software and hardware packages. The planned missions were then uploaded to the autopilot onboard the quadcopter which carried out the missions and returned safely to the launch site. All missions were conducted at an altitude of 50 m, within ±1.5 hours of solar noon to avoid deep shadows and bidirectional reflectance artifacts. The quadcopter was flown at a velocity of 3 m/s for all missions. Multiple flights were done over the season, but due to weather constraints and errors in stitched data only 2 days of good data collection, one mid-season and a second at the end of season (1: 08/02/2018, 2: 09/22/2018). The data from the sensors will be abbreviated as the name of the sensor and code of the date e.g. RE1 for Rededge-M data collected on 08/02/2018.

Ground Data

For verifying the performance of each sensor, leaf wilting scores were collected on each plot on multiple days of the season (King, 2009). Wilting scores were rated using a scale from 0-

Figure 3.3. a) Soybean crop used for data collection. b) Matrice 100 with a Sony α5100 CIR camera

100. 0 represented no wilting, 20 represented slight wilting evidence and rolling of leaves at top of the canopy, 40 represented severe rolling of leaves at the top of the canopy and moderate wilting of leaves throughout the plant, 60 represented severe wilting thought the canopy, 80 represented dead leaves throughout the canopy and severely wilted petioles and 100 represented plant death. The wilting scores collected 4 times during the season on 7/25, 08/01, 08/08 and 09/01/2018 will be abbreviated as W1, W2, W3 and W4 respectively. The most severe wilting scores were observed on 7/25. Scores for the latter three dates were relatively low because of more frequent rain events the second half of the season. Plant maturity was recorded as the number of days after August 31st when 95% of soybean pods have reached stage R8 (Christenson, 2013). After maturity, the center two rows of each plot was harvested to measure seed yield (kg/ha).

Sensor comparison

The quality of data extracted from the sUAS imagery depends greatly on the quality of the images collected. Other factors which play a role in producing quality data are image overlap, flight time, calibration, etc. For qualitative and quantitative analysis for comparing the different multispectral sensors the following experiments were performed with the aerial data collected:

Ground resolution

Aerial and satellite imagery have ground resolution often listed as a parameter for comparing between different sensors. According to Hengl (2006), at least four pixels are required to detect the smallest feature in an image. Therefore, it becomes necessary to look at ground resolution for the imagery collected in this study to compare the 2 infrared sensors. The ground resolution and the foot-print of the images collected for a flying altitude of 50 m was calculated for all the flights using ArcMap 10.4.1 (ArcGIS, ESRI, Redlands, CA, USA).

Statistical and orthomosaic analysis

Using the infrared imagery from both the sensors, one selected vegetative index was calculated. A Pigment Index (PI) was derived by subtracting the green normalized difference index (GNDVI) from the blue normalized difference index (BNDVI) (KSURF Invention Disclosure No.2016-010, 2016).

$$GNDVI = \frac{NIR - Green}{NIR + Green}$$

$$BNDVI = \frac{NIR - Blue}{NIR + Blue}$$

$$PI = BNDVI - GNDVI$$

During the process of photosynthesis plants produce reactive oxygen species as a secondary product along with sugars and fatty acids. High concentrations of reactive oxygen species are harmful to plants and stress causes these concentrations to increase (Hodecker et al., 2018; Kang et al., 2017). Also fungi and bacteria produce reactive oxygen species to invade plant tissues. To reduce the concentration of reactive oxygen, plants produce carotenoids which behave as antioxidants (Kim S. H. et al., 2012). Stress leads to higher carotenoid concentrations. Chlorophyll a and b absorb energy across blue and red regions of the electromagnetic spectrum whereas carotenoids absorb photons in the blue and green regions (Chappelle et al., 1992), as seen in Fig. 3.4 (Heliospectra, 2014). Also, plants reflect a considerable amount of energy in the NIR region of the spectrum. BNDVI values are influenced by chlorophyll a and b content with some influence of carotenoids. GNDVI is influenced by carotenoid concentration to a larger extent and is used to as a plant health indicator (Gitelson A. A. et al., 1996). PI values provide an indication of carotenoids to chlorophylls ratios, therefore it is correlated with stress conditions in the plant and physiological reasons that lead to changes in chlorophyll-carotenoid ratios, such as plant progression through growth stages (Hatton, 2018). A major advantage of the PI compared to other

types of spectral indices is that it decouples the influence of biomass from stress. NDVI provides low values even when the plant biomass is low. PI values are influenced less by biomass.

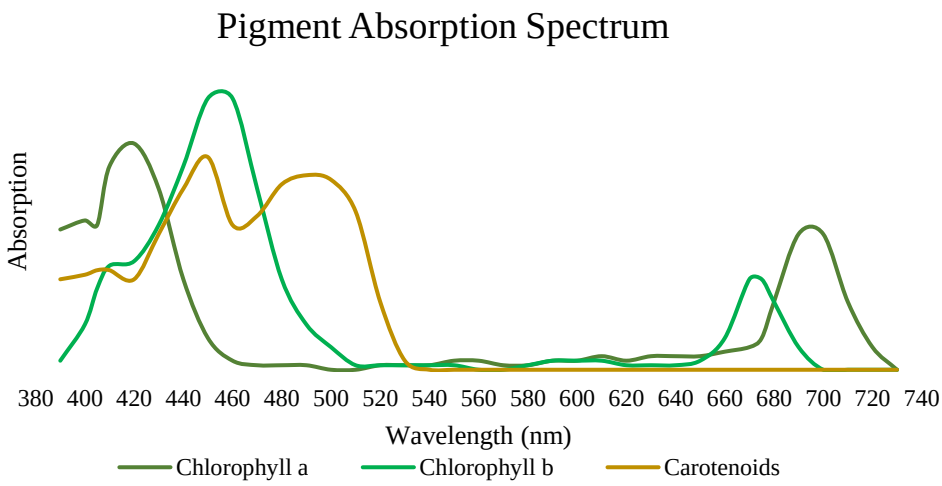

Figure 3.4. Plant Pigment spectral absorption distribution

PI index was extracted from the orthomosaics generated for each 4-row plot, only selecting the middle 2 plots to avoid errors due to pixel mixing. The PI was averaged into a single value for each 4-row plot. Anova analysis was done to check the differences between cultivars and sensors ability to identify differences in cultivars. Cultivar means were used to check significant differences between cultivars with respect to yield, maturity, S1, S2, RE1, RE2, F1, W1, W2, W3 and W4. A correlation matrix was created for checking the overall correlations between ground and aerial data (R Foundation, USA).

Results and Discussion

Ground resolution and spectral discrimination

The ground resolution (GR) and footprint (FP) from both the infrared sensors was calculated for a mission altitude of 50 m. The GR and FP for Sony α5100 were GR = 0.56 cm and FP = 33.6 x 22.3 m, whereas for Rededge-M they were GR = 3.47 cm and FP = 44.4 x 33.3 m. The Sony α5100 provided better ground resolution and footprint compared to Rededge-M which means more information is available from the imagery for spectral study (Fig. 3.5). Also there was a vast difference in sensor size between the Sony α5100 and Rededge-M. The Sony α5100 had a sensor size of 23.5 x 15.6 mm with 6000 x 4000 pixels on the sensor array. The Rededge-M had a sensor size of 4.8 x 3.6 mm with 1280 x 960 pixels on the sensor array. Rededge-M is a wide-angle camera (focal length = 5.4 mm) as compared to Sony α5100 (focal length = 16 mm). Sony α5100 16 mm lens is a less sharper lens due to this there are more number of pixels for transition between the 2 gradients. The results exhibited that Sony α5100 had better capability of gathering more detailed spatial information of the crop canopy which helps in understanding plants physiology. Rededge-M collected imagery in 16-bit (65,536 value intervals) radiometric resolution while the Sony α5100 imagery was collected with 8-bit (256 value intervals) radiometric resolution.

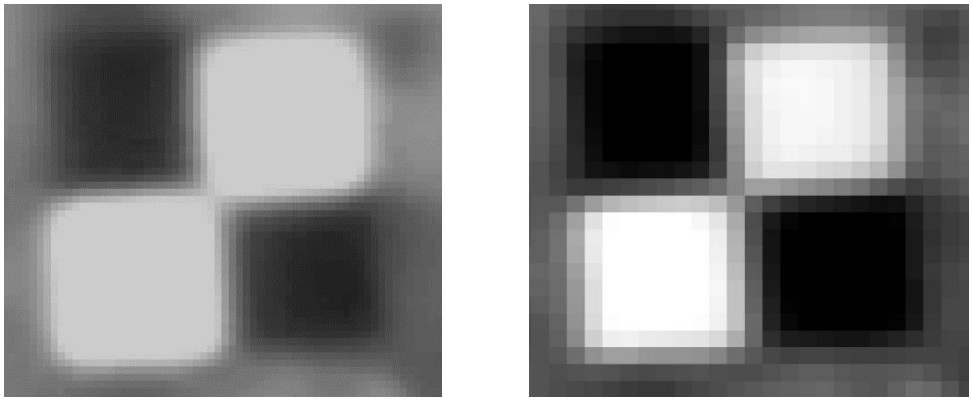

(a) (b)

Figure 3.5.Ground resolution comparison for a) Sony α5100 CIR and b) Rededge-M

Statistical and orthomosaic analysis

The orthomosaics created during this study were compared with each other (Fig. 3.6). The orthomosaics were created for the entire field not limited to the cultivars used for comparison. Similar patterns were found between imagery collected from S2, RE2 and F2. The pattern does not necessarily represent the cultivar differences. The areas in the close-up section of crop marked with the red boundary were areas where the plots spectrally exhibited poor health and areas marked with the green boundary were the areas that exhibited good health. These patterns indicate that even though different sensors were used in this study the spectral response of all the sensors somewhat remained similar. Further statistical comparison between camera sensors and ground data was done to fully evaluate the performance of the sensors.

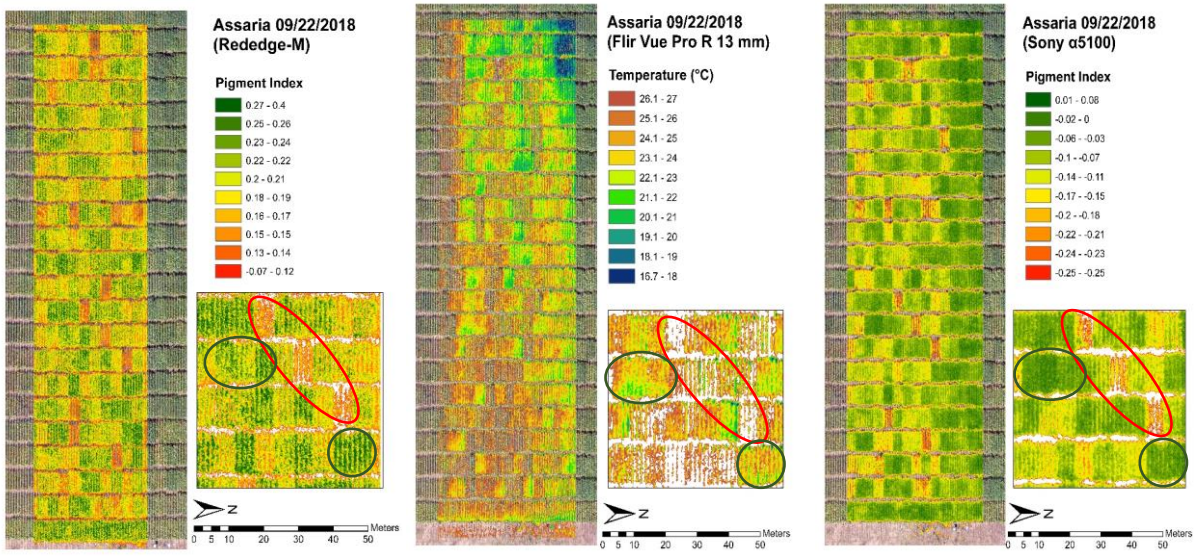

Figure 3.6.Orthomosaic generated with infrared imagery used in this study

Table 3.1 shows the F-values from analyses of variance for cultivar differences with respect to yield, maturity, S1, S2, RE1, RE2, F1, W1, W2, W3 and W4. Maturity S2, RE2 and W2 exhibited larger cultivar differences compared to the other variables. A correlation matrix (along with levels of significance) was created to evaluate the relationship between the phenotypic variables evaluated for cultivars (Tables 3.2 and 3.3). S2 was found to be highly correlated with

maturity ($r = 0.83$, $p \leq 0.001$). S2 was also correlated with yield ($r = 0.49$, $p \leq 0.01$). RE2 was only found to be significantly correlated to yield ($r = 0.63$, $p \leq 0.001$). Part of the correlation of S2 and RE2 with yield is due to later stages of crop maturity. Chlorophyll concentration decreases during senescing and stress no longer is reason for reduced chlorophyll activity. F2 showed correlation with maturity and S2 with r values of -0.68 ($p \leq 0.001$) and -0.61 ($p \leq 0.001$), respectively. Correlation between S1 with maturity and RE1 with S1 and S2 were significant but turned out to be small.S1 was found to have a correlation with maturity ($r = 0.47$, $p \leq 0.01$). RE1 was correlated to S1 and S2 with r values of 0.47 ($p \leq 0.01$) and 0.43 ($p \leq 0.05$) respectively.

Table 3.1. Analysis of variance summary for cultivar difference

	Y	MATURITY	S1	S2	RE1	RE2
F-VALUES	3.465***	60.762***	7.683***	59.415***	6.026***	30.077***
	F2	**W1**	**W2**	**W3**	**W4**	
F-VALUES	2.956***	10.8***	15.514***	2.029**	2.998***	

***** P = 0.001; ** P ≤ 0.01**

Significant correlations were observed between the wilting scores and the sensor data, but the correlations tended to be small, and varied in sign (Table 3.3) For example, a positive association was observed between W2 and S2 ($r = 0.42$, $p \leq 0.05$), while a negative association was observed between W3 and S1 ($r = -0.42$, $p \leq 0.05$). One possible reason for this inconsistency may have been related to the timing of the measurements. S2 was recorded later in the growing season than W2, when the plants were beginning to mature. S1 and W3 were recorded within 6 days of each other during pod fill and resulted in an expected negative correlation between PI and wilting, where cultivars with less wilting and under less stress tended to have higher PI values. However, in this data set, wilting scores were limited in their capability to discern differences among the cultivars and were not correlated to seed yield.

Table 3.2. Main effects means table for all the variables

ENTRY	YIELD	MATURITY	S1	S2	RE1	RE2	F2	W1	W2	W3	W4
E1	3104.5	27.5	-0.023	-0.143	0.071	0.191	23.2	36	3	11	14
E2	3388.9	29	-0.009	-0.105	0.080	0.219	23.7	33	3	10	9
E3	3628.7	30.25	-0.034	-0.110	0.066	0.220	24.1	31	14	15	21
E4	3172.4	28.75	-0.048	-0.100	0.068	0.205	23.7	51	34	23	18
E5	3543.6	34.75	-0.029	-0.052	0.074	0.235	22.9	41	13	13	13
E6	3595.5	38	-0.016	-0.043	0.090	0.206	22.8	43	25	19	15
E7	3657.1	41	-0.031	-0.057	0.081	0.189	22.0	29	11	9	18
E8	3129.1	25	-0.050	-0.139	0.072	0.191	23.7	36	14	18	9
E9	3717.8	37	-0.020	-0.042	0.101	0.226	23.8	55	48	18	24
E10	3039.9	46.5	-0.018	-0.027	0.055	0.146	21.6				3
E11	3509.9	28.75	-0.027	-0.064	0.077	0.238	23.9	46	30	23	28
E12	3352.9	41	-0.030	-0.063	0.085	0.190	22.5	26	11	9	21
E13	3063.9	26.25	-0.018	-0.154	0.070	0.188	23.4	28	0	9	18
E14	3672.0	32.25	-0.032	-0.107	0.075	0.229	25.3	36	13	14	29
E15	3698.8	29	-0.053	-0.085	0.059	0.215	23.1	50	41	19	33
E16	3433.0	29.75	-0.030	-0.068	0.089	0.231	24.0	49	33	20	15
E17	3174.0	32.25	-0.046	-0.096	0.081	0.235	24.6	41	18	19	26
E18	3443.9	41.5	-0.017	-0.047	0.088	0.183	21.5	63	48	19	33
E19	3570.1	32.5	-0.031	-0.098	0.084	0.234	24.4	36	13	13	33
E20	3622.8	33.75	-0.024	-0.055	0.076	0.235	23.3	45	11	11	10
E21	3774.8	40.75	-0.020	-0.041	0.089	0.202	22.8	35	16	16	33
E22	4027.3	35.75	-0.016	-0.041	0.078	0.244	21.8	35	13	11	16
E23	3642.1	29.5	-0.050	-0.096	0.074	0.215	23.0	49	18	19	39
E24	3380.2	27	-0.047	-0.124	0.069	0.199	23.9	41	24	15	35
E25	3309.4	27.5	-0.029	-0.140	0.074	0.192	25.1	23	3	11	31
E26	3457.5	28	-0.026	-0.135	0.078	0.192	24.4	20	1	9	20
E27	3663.8	27.25	-0.034	-0.140	0.060	0.196	24.2	23	6	9	20
E28	3581.6	32	-0.035	-0.066	0.069	0.231	23.0	53	35	17	28
E29	4105.8	35.25	-0.014	-0.054	0.090	0.246	23.8	45	26	11	36
E30	3957.5	35	-0.030	-0.045	0.081	0.245	22.0	31	18	11	20
E31	3762.1	40.5	-0.018	-0.026	0.082	0.228	22.7	28	5	18	18
E32	3572.2	38.75	-0.035	-0.048	0.082	0.222	23.3	54	38	20	31
E33	3651.0	35.75	-0.025	-0.052	0.076	0.230	23.7	35	26	13	16
E34	3772.7	28.5	-0.050	-0.086	0.062	0.212	24.6	55	43	19	23
E35	3511.0	39.75	-0.025	-0.063	0.082	0.199	22.0	23	5	10	10
MEAN	3533.92	33.314	-0.030	-0.080	0.077	0.213	23.37	38.8	19.1	14.6	21.7
VARIANCE	136332.4	31.052	0.000199	0.001464	0.000149	0.000546	2.59	154.2	228.7	46.0	169.0
CV	7.93	4.23	-28.69	-12.18	10.59	3.85	4.83	17.00	36.75	41.45	49.64
LSD (0.05)	393.08	1.979	0.0119	0.0137	0.01140	0.01151	1.58	9.3	9.9	8.5	15.1

Table 3.3. Correlation matrix for cultivar data

	MATURITY	S1	S2	RE1	RE2	F2	W1	W2	W3	W4
YIELD	0.24	0.15	0.49 **	0.31 .	0.63 ***	-0.1	0.09	0.22	-0.08	0.33 .
MATURITY		0.47 **	0.83 ***	0.39 *	-0.14	-0.68 ***	0.06	0.16	-0.05	-0.13
S1			0.37 *	0.47 **	0	-0.34 *	-0.23	-0.27	-0.42 *	-0.31 .
S2				0.43 *	0.28	-0.61 ***	0.35 *	0.42 *	0.24	-0.08
RE1					0.34 *	-0.11	0.15	0.18	0.05	0.19
RE2						0.24	0.25	0.2	0.18	0.23
F2							-0.05	-0.04	0.11	0.3 .
W1								0.88 ***	0.74 ***	0.34 .
W2									0.72 ***	0.38 .
W3										0.3 .

SIGNIF. CODES: '*' 0.001 '**' 0.01 '*' 0.05 '.' 0.1 ' ' 1**

Rededge-M was limited in its ability to calculate PI values. For fully observing the carotenoid activity with respect to chlorophyll, broad coverage of each color spectrum is required. In the methods, the chlorophyll and carotenoid overlapping electromagnetic spectrum activity was discussed. Sony α5100 being a broadband camera had overlapping bands and senses the full region in which the pigments are active. The Rededge-M is sensing a narrow region in the spectrum and no overlap is present between the bands. Rededge-M is therefore does not fully capture the pigment absorption spectrum for carotenoids.

Conclusions

Sony α5100 displayed better capability of gathering more detailed spatial information of the crop canopy. Overall anova and LSD means exhibited that the cultivars displayed maximum differences in means for maturity, S2, RE2 and W2. S2 was found highly correlated to maturity ($r = 0.83$, $p \leq 0.001$). Wilting scores were found limited in their ability to provide higher resolution data as compared with spectral data. With better resolution ground data the spectral responses can be confirmed as an actual crop parameter. Redegde-M was discovered to be restricted in its capacity to calculate the PI due to sensor limitation. In future studies, other vegetative indices

which can be derived from Rededge-M bands will be examined to check whether they correlate to crop parameters and ground data.

Chapter 4 - Impact of camera lens angle and sUAS flying altitude on spatial crop canopy temperature evaluation

Abstract

Thermal image quality is critical to accurately quantify spatial and temporal growth and stress patterns of field crops. Image data quality from a thermal sensor can be impacted by several factors including environment, flying altitude, and camera focal length. Often times the thermal sensor selection is based upon price or one already available for research. Metrics are available to select the flight altitude based on thermal sensor focal length for desired ground resolution, however, no study has been conducted to provide the relative difference in image data, quality and efficiency of generating a thermal orthomosaic. Therefore, this study was conducted with the goal to compare the accuracy of canopy temperature quantification and assess the quality of thermal orthomosaic when using a thermal sensor of different focal lengths and image acquisition at varying flying altitudes of an sUAS. Three thermal infrared cameras were selected with focal lengths of 9mm, 13mm, and 19mm. All three cameras were flown at altitudes of 20m, 50m, and 80m, to collect aerial imagery of a 7,000 m2 soybean field. The cameras were mounted on a rotary quadcopter. All flights were conducted at 3 m/s flying speed and 1 second shutter trigger interval. A ground reference system comprising of a panel and water bath system with measured actual temperature provided ground truth data for thermometric transformations. Imagery data were compared to assess differences in the number of images collected, percentage overlap required for 1 second shutter trigger interval, quality of orthomosaic and accuracy of canopy temperatures. Results showed that 13 mm focal length and 50 m altitude resulted in a finer resolution orthomosaic which can provide robust and accurate information on canopy temperature. The selection of such

a system of camera lens angle and altitude can provide accurate, reliable and rapid canopy temperature quantification..

Introduction

With the increasing human population, crop production must increase approximately 25-70 % from recent levels to meet demands in 2050 (Hunter et al., 2017). Sustainable agriculture is going to be a major contributing factor in achieving this goal. Sustainable agriculture is defined as the farming systems that can maintain their productivity and usefulness to society indefinitely. Such systems must be resource conserving, socially supportive, commercially competitive and environmentally sound (Ikerd, 1990). Precision agriculture is going to be a major contributor in creating a sustainable farming system. Precision agriculture is a farming practice in which farm inputs are optimized, overall efficiency of the farm is improved, and environmental footprint is reduced by concentrating on right management practice at right place at right time and at right rate (Gebbers and Adamchuk, 2010; Khanal et al., 2017; Hunt and Daughtry, 2018).

Remote sensing has been considered a crucial technology for precision agriculture (Robert, 1982; Mulla and Khosla, 2016; Moran, Inoue and Barnes, 1997; Brisco et al., 1998). Numerous research has been completed on remotely sensed data collected by satellite and aircraft platforms for agriculture purposes over the last 60 years (Colwell, 1956; Jackson, 1984; Pinter et al., 2003). In recent years, there has been an increase in the use of small Unmanned Aerial System(s) (sUAS) for remote sensing applications such as vegetation index calculations, species phenotyping, water stress identification, etc. (Berni et al., 2009; Baluja et al., 2012; Zaman-Allah et al., 2015; Senthilnath et al., 2017). UAS provide an alternate solution to traditionally used satellite and aircraft remote sensing. sUAS are more flexible to use in different climatic conditions and are economically affordable when compared to other remote sensing platforms (Zhang and Kovacs,

2012). In addition, the remotely sensed data can be obtained in higher resolution, especially for data based on the vegetation, which was not possible with traditional remote sensing platforms (Laliberte and Rango, 2011).

Different types of camera sensors are being used for remote sensing purposes. The selection of a camera is based on application, dimensional size, focal length, wavelengths observed, etc. The sensor types can be RGB true color, thermal infrared (TIR), multispectral broadband camera (MSB), multispectral camera, hyperspectral camera and other sensors (Majidi and Bab-Hadiashar, 2005; Berni et al, 2009; Zarco-Tejada et al., 2005; Kingston and Beard, 2004). The increase of sUAS use in crop fields has improved the process and response time of crop monitoring. MSB and TIR sensors are available from commercial manufacturers including DRS technologies, FLIR, AgEagle, Micasense and others, both for commercial and agricultural users.

Among these technologies, thermal camera sensors are gaining increased interest with researchers and farmers as a medium to determine plant health parameters (Bellvert, Marsal, Girona and Zarco-Tejada, 2014; Bellvert et al., 2014; Elvanidi et al, 2017; Ortega-Farías et al., 2016; Santesteban, 2017; Riberio-Gomes et al., 2017). Images collected by thermal sensors were used as an effective tool in the cultivation of potatoes to assess the water availability to the crop (Rud et al., 2014). Digital cameras along with thermal cameras were used to determine physiological data for vineyards with acceptable accuracy (Möller et al., 2007). In studies conducted on maize fields, thermometry was found useful in identifying plant stress by monitoring and quantifying water stress through measuring canopy temperature (DeJonge et al., 2015; and Mangus et. al., 2016). Thermal infrared sensors are also being used in other applications such as irrigation scheduling, soil moisture detection, drought stress monitoring and plant disease detection (Khanal et al, 2017; Nicholle et al, 2018).

Availability of a variety of sensors and platforms is good for any research application, however, it is critical to choose the correct sensor for the desired application. Before selecting a sensor, researchers consider data outcomes that are needed from the sensor. Common concerns that need to be answered are whether the spatial resolution is adequate to provide accurate and robust data for analytics and whether the images can be efficiently stitched to generate geometrically accurate orthomosaics. When using the thermal infrared spectrum, it is important to select a correct sensor as it is sensitive to atmospheric conditions like relative humidity, air temperature, wind speed and solar noon. These factors impact flying altitude selection, documenting environmental conditions and camera properties such as focal length or sensor size. Other factors which must be considered when comparing temporal data sets from test sites is the ability to segment canopy and robustness of canopy temperature extraction. Studies and matrices are available to determine ground resolution, but limited information is available on the factors affecting thermal infrared imagery collection. This study was designed to:

- Develop crop canopy thermal orthomosaic from aerial imagery collected at varying altitudes using thermal sensors of different focal lengths
- Conduct qualitative and quantitative analysis on different images and thermal orthomosaics.

Methods

sUAS and Cameras

A vertical take-off rotary copter quadcopter, Matrice – 100 (DJI, Shenzhen, China), was used to perform the low altitude aerial missions. The quadcopter can take off with maximum payload of 1 kg. The UAS has an in-built autopilot and missions which are custom made according to the application can be uploaded on the UAS using third party applications. UAS has compatibility to two batteries with each battery providing 5700mAh power to the copter, which

provides 25 minutes of effective flight time with thermal sensors (350 gm) onboard. The quadcopter is able to fly in wind speeds of up to 10 m/s but to assure safety standards and to avoid error in data due to wind influence, data was aquired when the wind speeds were less than 4.5 m/s. The sensors were mounted using a fixed gimbal on UAS.

The quadcopter was used to collect Thermal Infrared (TIR) data from TIR cameras (Flir Systems Inc, Wilsonville, OR, USA) with different lens characteristics. The focal lengths for the cameras used were 9 mm, 13 mm and 19 mm. All three TIR cameras had a standard VOx micro-bolometer sensor with 640x512 pixels and operated at 30 Hz of full frame rate. The spectral band observed by these cameras was 7-13.5 μm. The images were collected in a 14-bit tiff format. Using a tiff image instead of an 8-bit radiometric jpeg have advantages. The 8-bit radiometric Jpeg images are affected by the camera due to flat-field correction which occur whenever there is a difference between the temperature range the camera is observing. This causes the pixel values on the jpeg images to change even when the temperature of the observed feature does not change. The change in pixel values could create artifacts in an orthomosaic giving false information in the form of hot spots within the crop. The auto contrast correction does not happen when collecting tiff format images and this format also provides better radiometric resolution (14-bit) compared to a jpeg image format.

(a) (b)

Figure 4.1(a) The quadcopter platform with a mounted thermal infrared sensor (b) A close-up of the mounted sensor

Crop and Missions

The crop selected for this study was soybean. The plot area was approximately 7000 m2 and the soybean crop was at partial canopy closure. The plot was located southwest of the City of Manhattan, KS, in Kansas State University River Valley research farm at Ashland Bottoms (39.133028° N, -96.617874° W). The trails were on progeny varieties of soybeans developed in Kansas State University. The varieties were planted in 1-row plots, 2 m long and 0.76 m apart. The soil type of the filed was Bismarckgrove - Kimo complex. The missions were created on Mission Planner (Mission Planner®, by Michel Oborne) autopilot software suite. Mission Planner was used as a configuration utility and also as a dynamic control supplement for compatible autonomous vehicles. After determining the mission characteristics, the mission files were then imported into a third party autonomous flight application (Litchi® for DJI). Litchi allowed mission files from Mission Planner to be uploaded onto the quadcopter. This functionality is not available within DJI software and hardware packages. The planned missions were then uploaded to the autopilot present onboard the quadcopter which carried out the mission and returned safely to the launch site. Missions were planned to collect aerial imagery at three different altitudes of 20 m, 50 m and 80 m. All the missions were conducted within ±1.5 hours of solar noon to avoid deep shadows and unevenly heated plants. Additional preliminary studies conducted during the project indicated that neglecting to fly within the solar noon window could potentially create artifacts (inaccurate canopy temperature quantification) and software stitching errors. The quadcopter was flown at a velocity of 3 m/s for all of the missions. The velocity was carefully chosen after initial experimentation with various aircraft velocities. The quadcopter was flown at speeds ranging from 2 to 5 m/s. At the speeds of 4 and 5 m/s and flying at lower altitudes, the sensor needed to have a trigger frequency of less than 1 sec which was not possible with the available TIR cameras and the

images obtained at these speeds were blurry. At the speed of 2 m/s the flight time for some flights exceeded the quadcopter's capability to complete the mission before running out of battery power.

Ground truthing

Using thermal infrared sensors requires temperature calibration to account for atmospheric variations so that the quantification of crop canopy temperature is done correctly. In this study, a custom-made weather station was developed with an integrated data acquisition (DAQ) system and environmental sensor package data using a NI myRIO (National Instruments, Austin, TX, USA) for calibration of thermal imagery to correct temperature values. The weather station was designed to have different temperature gradients on matte painted metal panels having emissivity values ranging from 088-0.93, which provided a range of maximum and minimum temperatures that were present when the flight was being conducted. The temperature of these panels was constantly recorded using thermistors (Precision Thermistor Element, 44004, Omega Engineering, Norwalk, CT, USA). A relationship was established between the Dn (digital number) values which extracted from orthomosaics using ArcMap 10.4.1 (ArcGIS, ESRI, Redlands, CA, USA) and temperature recorded from the weather station to apply the thermometric transformation to each orthomosaic. The temperature points are plotted against Dn and regression equation is estimated using the data. Then the data is plotted against the regression equation and the points continually followed the regression line validating that the calibration curve is highly accurate.

Figure 4.2 Ground truthing station for calibrating thermal imagery

Image quality comparison

The quality of data extracted from the sUAS imagery depend greatly on the quality of the images collected. Other factors which play a role in producing quality data are image overlap, flight time, geometric accuracy, etc. For qualitatively and quantitatively comparing images and orthomosaics from the various flights of this study, a variety of parameters were selected by referencing a previous study that was conducted to assess quadcopter image quality at different altitudes (Mesas-Carrascosa et al., 2015). The images and orthomosaics were evaluated on the following parameters:

Non-Reference Image Quality Metrics (NRIQM)

Image visual quality is always an important factor while evaluating aerial imagery. In this study image scores were calculated which indicated the relative quality of the images. NRIQM scores were calculated using Matlab (2018a), for Natural image Quality Evaluator (NIQE) (Mittal et al., 2013) and Blind/Referenceless Image Spatial Quality Evaluator (BRISQUE) (Mittal et al., 2012). Both NIQE and BRISQUE are metrics developed by image quality researchers which use Natural Scene Statistics (NSS) to score image quality. BRISQUE is an opinion aware model, which means that this model is trained with a known database of good quality images whereas NIQE is an opinion unaware model meaning it is not trained using a database. Image quality scores were calculated and averaged for each flight for comparison. The score for a good quality image will be lower than the score for a poor quality image for both NIQE and BRISQUE.

Geometric Accuracy

Aerial imagery is useful if it is geometrically accurate and is able locate the region in study correctly on map, thus making it a critical parameter while comparing different orthomosaics. The method used for calculating geometric accuracy was the Root Mean Square Error (RMSE) method

suggested by the American Society for Photogrammetry and Remote Sensing (ASPRS). RMSE is defined as the error in the square root of the average of the squared discrepancies. For calculating geometric accuracy a large black and white checkerboard patterned sheet with an individual square size of 30.48 x 30.48 cm was built (Fig. 4.3). The vertices of the square blocks were marked as checkpoints. Real-Time Kinematic (RTK) corrected GPS coordinates were collected and assigned to each checkpoint. The GPS position coordinates from the orthomosaics were then extracted from the orthomosaic for an error calculation and comparison with the actual position coordinates of the checkpoint. The error was calculated in both north – south and east – west directions namely RMSEy and RMSEx, then RMSE was compared across the collection of flights. Lower RMSE values indicated a better geometric accuracy within the generated orthomosaics which improves data manipulation and utilization within production agriculture.

Figure 4.3 Checkerboard used for calculating RMSE for geometric accuracy

Ground Resolution and Spectral Discrimination

Aerial and satellite imagery have ground resolution often listed as a parameter for comparing between different sensors. At least 10 pixels are required to report a meaningful thermal measurement (Flir Technical Note, 2016). Therefore, it becomes necessary to select an altitude which provides a fine ground resolution. For this study the ground resolution and the foot-print of

the images collected was calculated for all the conducted flights using ArcMap 10.4.1 (ArcGIS, ESRI, Redlands, CA, USA).

In order to access if the resolution was sufficient to identify crop from soil, spectral discrimination was determined for all the orthomosaics. Spectral discrimination is defined as how well the image pixels are able to differentiate between two different features or between foreground and background. Spectral discrimination plots were made by extracting pixel values across the colored wooden panels using ArcMap (Fig. 4.4), which should exhibit a parabola in the center indicating a sudden jump in the pixel values. Depending upon how sharp the slope of the approaching line is to the peak, conclusions can be drawn to determine how well the pixels were spectrally discriminated. The sharper the slope of the approach, the better the spectral discrimination exhibited by the camera.

Canopy Temperature Extraction from Thermal Orthomosaics

Numerous software platforms are available to generate orthomosaics from sUAS imagery. For this study the collected thermal imagery was stitched using Metashape (Agisoft Metashape, Agisoft LLC, St. Petersburg, Russia). Metashape was selected as it provides more freedom in selecting stitching parameters and is more flexible in working with imagery from any camera. The stitched imagery was exported as an orthomosaic having a .tiff file extension. The thermal orthomosaics were generated using the exported orthomosaics with ArcMap 10.4.1 (ArcGIS, ESRI, Redlands, CA, USA) to observe the canopy temperature distribution for the crop across different flights. A temperature curve made from the weather station data was used to calibrate the thermal orthomosaics. Canopy temperatures were extracted from the orthomosaics using 3D analyst tool in ArcMap.

Figure 4.4 Wooden panels used to measure spectral discrimination

Results and Discussion

Non-Reference Image Quality Metrics (NRIQM) and Geometric Accuracy

The NRIQM scores did not show any large deflections from each other, indicating that there was little impact on the quality of image irrespective of chosen flying altitude and focal length of the camera (Table 4.1). This means image quality is independent of parameters usually considered before selecting a sensor for data collection.

Geometric accuracy results (Table 4.2) indicated that the 9 mm thermal sensor at an altitude of 80 m presented the highest value of RMSE both in terms of longitude (RMSEx = 0.191 m) and latitude (RMSEy = 0.344 m). Overall, the lowest RMSE values for both directions (RMSEx = 0.031 m, RMSEy = 0.034 m) were observed when using the 13 mm thermal sensor at an altitude of 20 m. For RMSE in the x direction, the lowest RMSE was observed for 19 mm thermal sensor at an altitude of 50 m, whereas the lowest RMSE for the y direction was exhibited by 13 mm thermal sensor at an altitude of 20 m. Lower RMSE means better ability of the orthomosaic to accurately represent the original position of the features present in the orthomosaic.

Table 4.1 NIQE and BRISQUE scores for images taken from all the flight combinations

FOCAL LENGTH	IMAGE QUALITY INDICATOR	ALTITUDE		
		20 m	50 m	80 m
9 MM	NIQE	Avg: 10.2	Avg: 9.4	Avg: 8.7
	BRISQUE	Avg: 47.0	Avg: 46.4	Avg: 46.7
13 MM	NIQE	Avg: 10.3	Avg: 10.9	Avg: 9.6
	BRISQUE	Avg: 46.9	Avg: 46.5	Avg: 45.8
19 MM	NIQE	Avg: 10.4	Avg: 10.4	Avg: 10.6
	BRISQUE	Avg: 48.4	Avg: 46.7	Avg: 45.7

Table 4.2 RMSEx and RMSEy values for all the flight combinations

	20 M		50M		80M	
	RMSEx	RMSEy	RMSEx	RMSEy	RMSEx	RMSEy
9MM	0.028	0.053	0.030	0.094	0.191	0.344
13MM	0.031	0.034	0.047	0.045	0.053	0.043
19MM	0.041	0.038	0.028	0.047	0.043	0.050

Ground Resolution and Spectral Discrimination

Ground Resolution (GR) and footprint (FP) for all the flights of thermal sensors was noted and arranged in a metric (Table 4.3). The smallest GR and FP was exhibited by the 19 mm thermal sensor at an altitude of 20 m: GR = 1.79 cm and FP = 11.5 x 9.2 m. Also, the highest GR and FP was exhibited by the 9 mm thermal sensor at an altitude of 80 m: GR = 15.11 cm and FP = 96.7 x 77.4 m..

Table 4.3 Ground resolution and footprint in parenthesis for all the focal length of the thermal sensors at different flying altitudes

	ALTITUDE		
FOCAL LENGTH ↓	20 m	50 m	80 m
9 MM	3.78 cm (24.2 x 19.3 m)	9.44 cm (60.4 x 48.4 m)	15.11 cm (96.7 x 77.4 m)
13 MM	2.62 cm (16.7 x 13.4 m)	6.54 cm (41.8 x 33.5 m)	10.46 cm (67 x 53.6 m)
19 MM	1.79 cm (11.5 x 9.2 m)	4.47 cm (28.6 x 22.9 m)	16 cm (745.8 x 36.6 m)

The GR and FP data also showed that the type of information to be extracted from a raster could a major factor in deciding the focal length and flying altitude. Depending on the size of the canopy and the size of the plant leaf it would be important to know the extent of information on a single pixel. If the pixel size is bigger than the canopy, then the information coming into that pixel is diluted by the background and may not accurately represent actual canopy temperature. Similarly, there should be a minimum of 10 pixels on the canopy to accurately extract canopy emittance or temperature. To access the accuracy of canopy temperature, an analysis was conducted on a segmented image of a 60.96 x 60.96 cm ground control point from each orthomosaic (Figure 4.5).

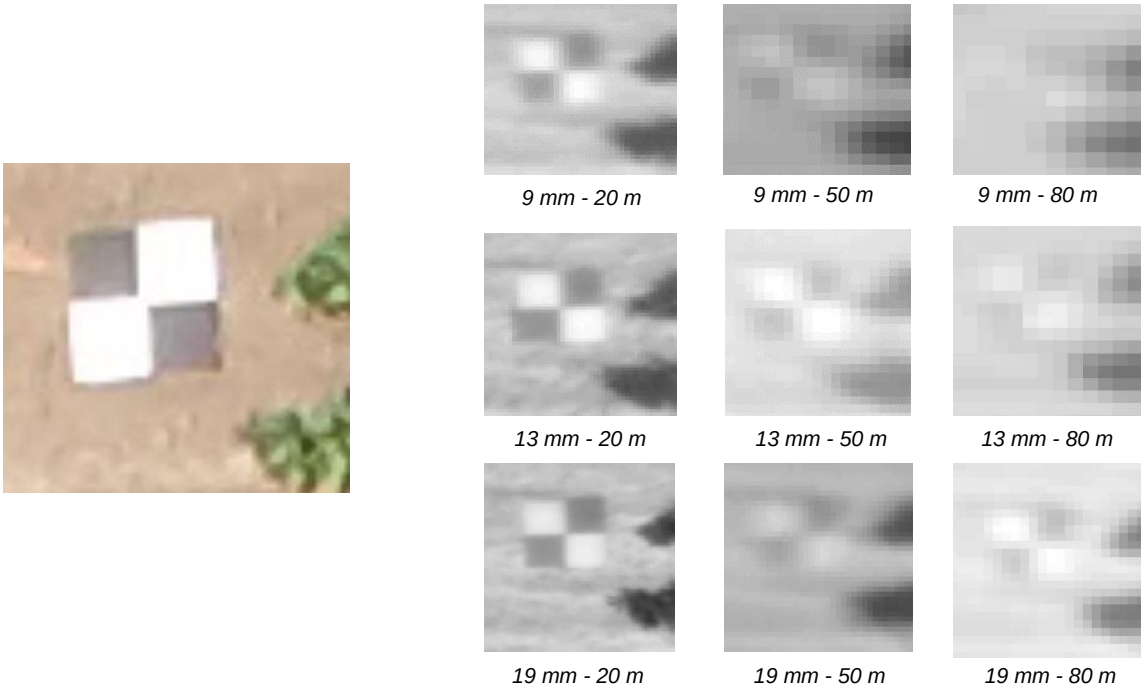

Figure 4.5. on the left is the ground control point from visible camera which was used to compare ground resolution for each flight combination. On the right are the segmented images from the thermal orthomosaics of the same ground control point at the different resolutions

Figure 4.5 shows a clear visual differentiation between ground resolution results and orthomosaics and also indication of orthomosaics from which more accurate canopy temperature information could be extracted. Features are not distinguishable for 9 mm thermal sensor at a flying

altitude of 80 m, and there is no difference between soil pixels, panel pixels or plant pixels. Similarly, the 19 mm thermal sensor at flying altitude of 20 m resulted in distinguishable soil, panel, and plant pixels. Figure 4.6 contains the spectral discrimination plots collected in the study. An acceptable plot will be one which has the ascending and descending slope almost perpendicular to the x-axis and a flat response at the top of the plot representing enough number of pixels present on the panel. The more gradual the slope, lesser the ability of the camera to spectrally separate features in an image. Also less number of pixels on panel due to poor resolution indicate fewer information available from pixels and possibility of pixel mixing in the imagery. Results indicate that all plots surpassed the threshold that justified them as acceptable except all 80 m altitude

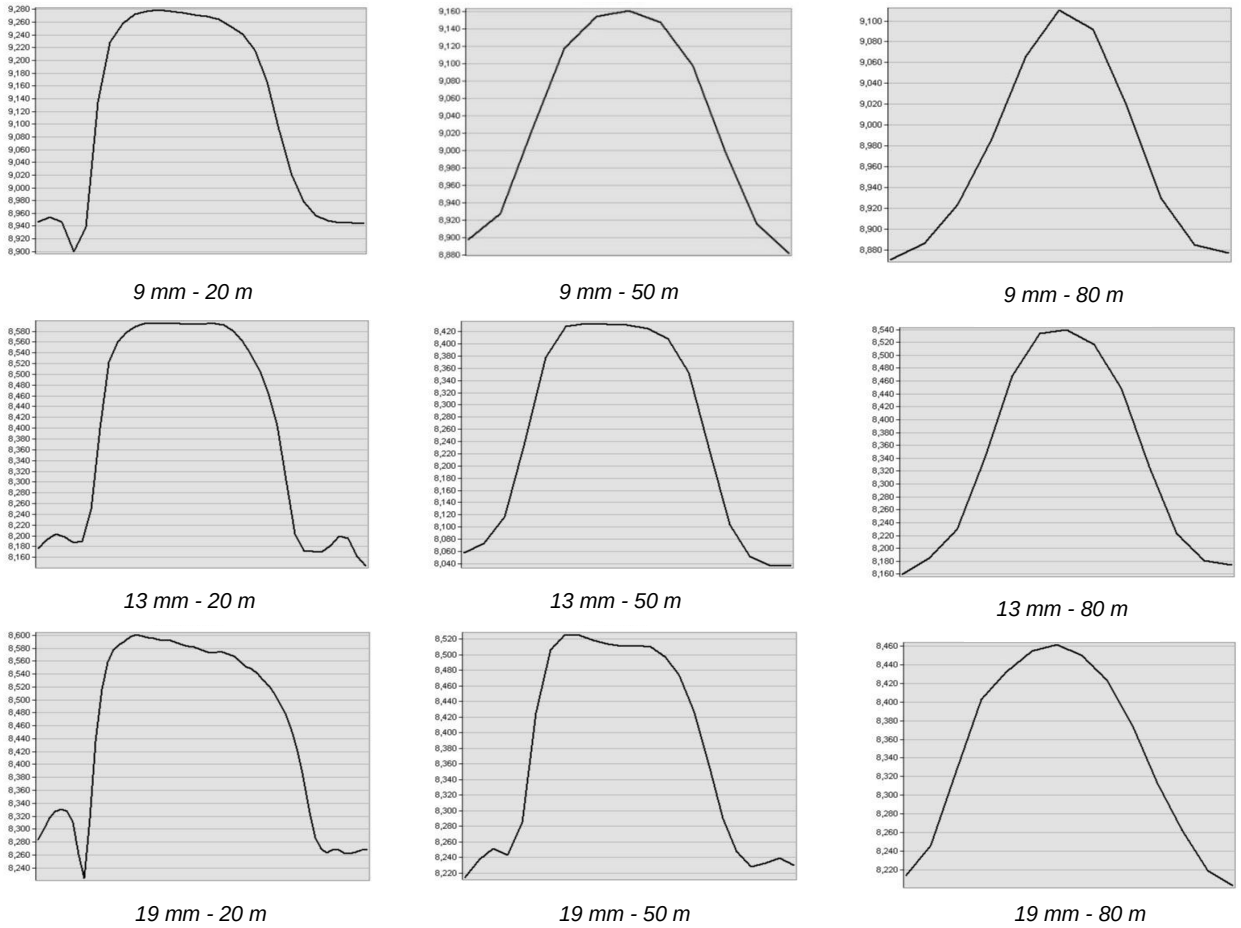

Figure 4.6 Spectral discrimination plots for the thermal sensors flown at different altitudes

flights and one 50 m using the 9 mm thermal sensor flight which did not presented acceptable discrimination in the pixels.

Flight Time and Image Overlap

Flying at very low altitude may provide higher resolution and better spectral discrimination but low altitude flights are limiting due to longer flight time to cover even smaller number of acres and limitation of battery life to complete a single flight (25 mins) with needed sensor payloads. Additionally, users may have to select an overlap (both side-to-side and back-to-forth) which would be less than the recommended overlap (≥ 80 %) by commercial software's (Table 4.4). The lower image overlaps causes issues during image processing as it becomes difficult for the software to find common features between images to be able to stitch images together. The most common concerns with lower image overlap was the potential impact of the change in weather from start to finish of flight on canopy emittance and insufficient common tie points to build a dense cloud for the edge of the test plot. Overall, users must consider the trade-off between flight time and altitude for appropriate image overlap to develop more accurate orthomosaics.

Table 4.4 Flight time and image overlaps used for each thermal sensor at different altitudes

	20 M	50 M	80 M
9 MM	14 mins 80 % front lap 80 % side lap	11 mins 90 % front lap 89 % side lap	9 mins 90 % front lap 89 % side lap
13 MM	22 mins 76 % front lap 79 % side lap	11 mins 85 % front lap 85 % side lap	11 mins 90 % front lap 90 % side lap
19 MM	22 mins 66 % front lap 70 % side lap	17 mins 85 % front lap 85 % side lap	11 mins 87 % front lap 82 % side lap

Thermal Orthomosaic

Results from this study showed that all the thermal orthomosaics had an even temperature distribution over the canopy and no artifacts were observed. As an example, two of the orthomosaics are shown in Figure 4.7 with cropped thermal maps highlighting 4-row plots. Within

a 4-row plot, the role of ground resolution and spectral discrimination becomes very evident. In the flight at an altitude of 50 m with 13 mm thermal sensor, results showed a distinct separation between soil and canopy pixels. The number of pixels in the center of the canopy was close to 100 and not affected by the soil background. The results indicated that there was sufficient and accurate information available which was not diluted by the surrounding surfaces. However, during the mission at 80 m with 9 mm thermal sensor the differentiation between the soil and canopy pixels was not discrete. The discrete distinction was due to not enough number of pixels within the canopy (close to 10), which potentially could result in data extraction difficult and if not conducted correctly data may not accurately representing true canopy temperature. Canopy temperatures extracted carefully from the thermal orthomosaics and compared to the plant temperature collected using a Flir TG167 (Flir Systems Inc, Wilsonville, OR, USA) held at 30 cm above the crop canopy exhibited that the plant temperature during the flight captured by the thermal infrared sensors were with an error range of ±1° C as compared with ground data (table 4.5) ($t = 0.92609$, p-value = 0.3767). The results indicated that thermal sensor can accurately capture canopy temperature on spatial scale accurately ($r = 0.84$, $p = 0.036$).

Table 4.5 Sample temperature readings from crop canopy collected from Flir TG167 and 13 mm 50 m thermal orthomosaic

	FLIR TG167	13 MM 50 M
C1	31.8	30.9
C2	33.1	32.32
C3	31.7	30.52
C4	32.2	31.45
C5	30.2	30.9
C6	29.9	29.17

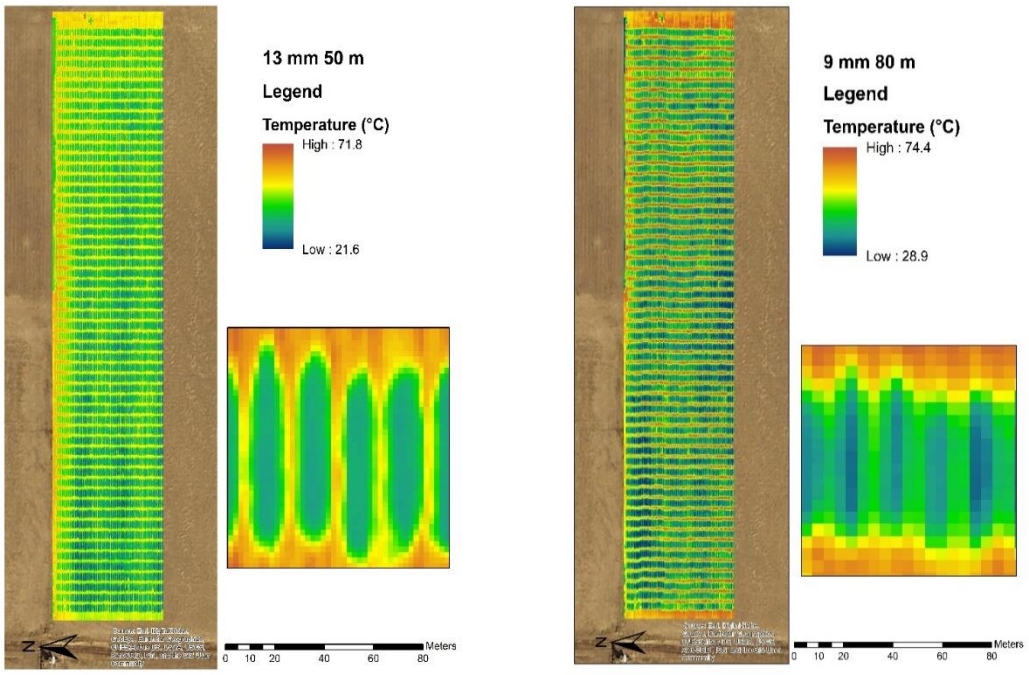

Figure 4.7 Thermal orthomosaic map generated for 13 mm and 9 mm focal length thermal sensors at flying altitude of 50 m and 80 m

Conclusion and future work

According to our experimental study, the 13 mm thermal infrared camera at 50 m provided appropriate image overlap, spectral discrimination, flying time trade-off, ground resolution, image quality, and accurate crop canopy temperatures. In the orthomosaic generated from this set of images, there was enough number of pixels to extract valuable data from the crop canopy. In particular, the RMSE in geometric accuracy was low and consistent in both directions. Other flight combinations also performed well in some criteria but using the images from these flights may require extensive post-processing to able to extract data. Future studies will be conducted on different crops like corn, wheat, sorghum, etc. to see the effect of the change in crop canopy on the listed parameter on this study.

Chapter 5 - Conclusion

Summary of finding

Remote sensing applications using sUAS in agricultural industry are growing day by day. Different kind of spectral sensors can be used onboard sUAS with great efficiency. But it was noticed that the sensors used in these studies were the one which were already available with the researcher or which are easily available commercially. Consideration was not given to examine and compare specifications related to each sensor, such as sensor size and radiometric resolution. Also other sUAS parameters such as flying altitude and flight speed were not properly evaluated. There is a need to understand these parameters to expand the knowledge which is available regarding sUAS and sensors used onboard them. This information can improve the quality of data collected on crops using sUAS sensors. In this thesis thermal infrared, modified color infrared and multispectral sensors were identified and compared based on the parameters specific to the sensor involved, to understand and improve future selection of sUAS sensors.

Sony α5100 displayed better capability of gathering more detailed spatial information of the crop canopy. Sony α5100 was found highly correlated to maturity ($r = 0.83$, $p \leq 0.001$). Wilting scores were found limited in their ability to provide higher resolution data as compared with spectral data. With better resolution ground data the spectral responses can be confirmed as an actual crop parameter. Redegde-M was discovered to be restricted in its capacity to calculate the PI due to sensor limitation. In future studies, other vegetative indices which can be derived from Rededge-M bands will be examined to check whether they correlate to crop parameters and ground data.

The 13 mm thermal infrared camera at 50 m flying altitude provided appropriate image overlap, spectral discrimination, flying time trade-off, ground resolution, image quality, and

accurate crop canopy temperatures. In the orthomosaic generated from this set of images, there was enough number of pixels to extract valuable data from the crop canopy. In particular, the root mean square error in geometric accuracy was low and consistent in both directions. Other flight combinations also performed well in some criteria but using the images from these flights may require extensive post-processing to able to extract data. Future studies will be conducted on different crops like corn, wheat, sorghum, etc. to see the effect of the change in crop canopy on the listed parameter on this study.

References

Aasen, H., Burkart, A., Bolten, A., and Bareth, G. (2015). Generating 3D hyperspectral information with lightweight UAV snapshot cameras for vegetation monitoring: from camera calibration to quality assurance. Isprs J. Photogram. Remote Sensing 108, 245–259. doi: 10.1016/j.isprsjprs.2015. 08.002

Adão, T. et al. (2017) Hyperspectral imaging: a review on UAV-based sensors, data processing and applications for agriculture and forestry. Remote Sens. 9, 1110

Alexandridis, T. et al. (2017) Novelty detection classifiers in weed mapping: Silybum marianum detection on UAV multispectral images. Sensors 17, 2007

Arthur, A. M., & Robinson, I. (2015). A critique of field spectroscopy and the challenges and opportunities it presents for remote sensing for agriculture, ecosystems, and hydrology. Remote Sensing for Agriculture, Ecosystems, and Hydrology XVII, , 9637

Baluja, J., Diago, M.P., Balda, P., Zorer, R., Meggio, F., Morales, F., Tardaguila, J., (2012) Assessment of vineyard water status variability by thermal and multispectral imagery using an unmanned aerial vehicle (UAV). Irrigation Science. 30, 511–522.

Bareth, G., Bendig, J., Tilly, N., Hoffmeister, D., Aasen, H., and Bolten, A. (2016). A Comparison of UAV- and TLS-derived plant height for crop monitoring: using polygon grids for the analysis of crop surface models (CSMs). Photogrammetrie Fernerkundung Geoinformation 2016, 85–94. doi: 10.1127/pfg/2016/0289

Beard, R. W., Kingston, D., Quigley, M., Snyder, D., Christiansen, R., Johnson, W., . . . Goodrich, M. (2005). Autonomous vehicle technologies for small fixed-wing UAVs. Journal of Aerospace Computing, Information, and Communication, 2(1), 92-108.

Bellvert, J., Marsal, J., Girona, J., Zarco-Tejada, P.J., (2014). Seasonal evolution of crop water stress index in grapevine varieties determined with high-resolution remote sensing thermal imagery. Irrigation Science. 33, 81–93.

Bellvert, J., Zarco-Tejada, P.J., Girona, J., Fereres, E., (2014). Mapping crop water stress index in a “Pinot-noir”vineyard: Comparing ground measurements with thermal remote sensing imagery from an unmanned aerial vehicle. Precision Agriculture. 15, 361–376.

Bendig, J. et al. (2015) Combining UAV-based plant height from crop surface models, visible, and near infrared vegetation indi-ces for biomass monitoring in barley. Int. J. Appl. Earth Obs. Geoinf. 39, 79–87

Berni, J.A.J. et al. (2009) Mapping canopy conductance and CWSI in olive orchards using high resolution thermal remote sensing imagery. Remote Sens. Environ. 113, 2380–2388

Berni, J.A.J., Zarco-Tejada, P.J., Suárez, L., Fereres, E., (2009) Thermal and narrowband multispectral remote sensing for vegetation monitoring from an unmanned aerial vehicle. IEEE Trans. Geoscience Remote Sensing 47,722–738.

Berra, E.F. et al. (2017) Commercial off-the-shelf digital cameras on unmanned aerial vehicles for multitemporal monitoring of vegetation reflectance and NDVI. IEEE Trans. Geosci. Remote Sens. 55, 4878–4886

Booth, D. T., Cox, S. E., Fifield, C., Phillips, M., andWilliamson, N. (2005). Image analysis compared with other methods for measuring ground cover. Arid Land Res. Manag. 19, 91–100. doi: 10.1080/15324980590916486

Brisco, B., Brown, R. J., Hirose, T., McNairn, H., Staenz. K., (1998). Precision Agriculture and the Role of Remote Sensing: A Review. Canadian Journal of Remote Sensing 24 (3): 315–327. doi:10.1080/07038992.1998.10855254.

Brocks, S. and Bareth, G. (2018) Estimating barley biomass with crop surface models from oblique RGB imagery. Remote Sens. 10, 268

Bureau, U. S. C. (2011). International Data Base, World Population: 1950-2050. June, 8, from https://www.census.gov/population/international/data/idb/worldpopgraph.php

Burkart, A. et al. (2018) Phenological analysis of unmanned aerial vehicle based time series of barley imagery with high temporal resolution. Precis. Agric. 19, 134–146

Candiago, S., Remondino, F., Giglio, M. D., & Gattelli, M. (2015). Evaluating multispectral images and vegetation indices for precision farming applications from UAV images. Remote Sensing, 7, 4026-4047.

Chapman, S., Merz, T., Chan, A., Jackway, P., Hrabar, S., Dreccer, M., et al. (2014). Pheno-Copter: a low-altitude, autonomous remote-sensing robotic helicopter for high-throughput field-based phenotyping. Agronomy 4, 279–301. doi: 10.3390/agronomy4020279

Chappelle, E. W., Kim, M. S., & Mcmurtrey, J. E. (1992). Ratio analysis of reflectance spectra (RARS): An algorithm for the remote estimation of the concentrations of chlorophyll A, chlorophyll B, and carotenoids in soybean leaves. Remote Sensing of Environment, 39(3), 239-247. doi:10.1016/0034-4257(92)90089-3

Chu, T. et al. (2016) Cotton growth modeling and assessment using unmanned aircraft system visual-band imagery. J. Appl. Remote Sens. 10, 036018

Chu, T.X. et al. (2017) Assessing lodging severity over an experimental maize (Zea mays L.) field using UAS images. Remote Sens. 9, 923

Chlingaryan, A. et al. (2018) Machine learning approaches for crop yield prediction and nitrogen status estimation in precision agriculture: a review. Comput. Electron. Agric. 151, 61–69

Christenson, B. S., (2013). Kansas State University, Degree Granting Institution. Characterization of Soybean Seed Yield Using Optimized Phenotyping. 2013. Web.

Colomina, I. and Molina, P. (2014) Unmanned aerial systems for photogrammetry and remote sensing: a review. ISPRS J. Photo-gramm. Remote Sens. 92, 79–97

Colwell, R. (1956). Determining the Prevalence of Certain Cereal Crop Diseases by Means of Aerial Photography. Hilgardia 26 (5): 223–286. doi:10.3733/hilg.v26n05p223.

Corcoles, J. I.,Ortega, J. F., Hernandez,D., andMoreno,M. A. (2013).Use of digital photography fromunmanned aerial vehicles for estimation of leaf area index in onion (Allium cepa L.) (Retracted article. See vol. 51, pg. 140, 2013). Eur. J. Agron. 45, 96–104. doi: 10.1016/j.eja.2012.11.001

Crimmins A. (2016). The impact of climate change on human health in the United States: a scientific assessment. Global Change Research Program, Washington, 190-205

de Castro, A.I. et al. (2018) An automatic random forest-OBIA algorithm for early weed mapping between and within crop rows using UAV Imagery. Remote Sens. 10, 285

DeJonge, K. C., Taghvaeian, S., Trout, T. J., Comas, L.H., (2015) Comparison of canopy temperature-based water stress indices for maize. Agricultural Water Management. 156, 51–62.

Diaz-Varela, R.A. et al. (2015) High-resolution airborne UAV imagery to assess olive tree crown parameters using 3D photo reconstruction: application in breeding trials. Remote Sens. 7, 4213–4232

Dillen, M. et al. (2016) Productivity, stand dynamics and the selection effect in a mixed willow clone short rotation coppice plantation. Biomass Bioenergy 87, 46–54

Ding, K. (2018) State of knowledge of irrigation techniques and practicalities within given socio-economic settings. Irrig. Drain. Published online March 25, 2018. http://dx.doi.org/10.1002/ ird.2237 13.

Du, M.M. and Noguchi, N. (2017) Monitoring of wheat growth status and mapping of wheat yield's within-field spatial varia-tions using color images acquired from UAV-camera system. Remote Sens. 9, 289

Ehsani, R., Sankaran, S., Maja, J., & Neto, J. C. (2014). Affordable multi-rotor remote sensing platform for applications in precision horticulture. Paper presented at the 12th International Conference on Precision Agriculture.

Elvanidi, A., Katsoulas, N., Bartzanas, T., Ferentinos, K.P., Kittas, C. (2017). Crop water status assessment in controlled environment using crop reflectance and temperature measurements. Precision Agriculture. 332–349.

Everaerts, J. (2008). The use of unmanned aerial vehicles (UAVs) for remote sensing and mapping. The International Archives of the Photogrammetry, Remote Sensing and Spatial Information Sciences, 37, 1187-1192.

Flir Technical Note, 2016. www.flir.com/suas.

Gago, J. et al. (2015) UAVs challenge to assess water stress for sustainable agriculture. Agric. Water Manag. 153, 9–19 15.

Gago, J. et al. (2017) Integrative field scale phenotyping for investigating metabolic components of water stress within a vineyard. Plant Methods 13, 1–14

Gracia-Romero, A. et al. (2017) Comparative performance of ground vs. aerially assessed RGB and multispectral indices for early-growth evaluation of maize performance under phospho-rus fertilization. Front. Plant Sci. 8, 2004

Garcia-Ruiz, F., Sankaran, S., Maja, J. M., Lee, W. S., Rasmussen, J., & Ehsani, R. (2013). Comparison of two aerial imaging platforms for identification of Huanglongbing-infected citrus trees. Computers and Electronics in Agriculture, 91, 106-115. doi:https://doi.org/10.1016/j.compag.2012.12.002

Gebbers, R., Adamchuk, V.I., 2010. Precision agriculture and food security. Science 327, 828–831.

Geipel, J., Link, J., and Claupein, W. (2014). Combined spectral and spatial modeling of corn yield based on aerial images and crop surface models acquired with an unmanned aircraft system. Remote Sensing 6, 10335–10355. doi: 10.3390/rs61110335

Gitelson, A. A., Kaufman, Y. J., & Merzlyak, M. N. (1996). Use of a green channel in remote sensing of global vegetation from EOS- MODIS. Remote Sensing of Environment, 58(3), 289-298. doi:10.1016/S0034-4257(96)00072-7.

Hatton, N. M., (2018). Use of small unmanned aerial system for validation of sudden death syndrome in soybean through multispectral and thermal remote sensing. 2018. Web.

Hatton, N., Sharda, A., Schapaugh, W., Merwe, D. V. D. (2018). Remote thermal infrared imaging for rapid screening of sudden death syndrome in soybean. 2018 ASABE Annual International Meeting. Paper No. 1800881, pages 1-22 (doi: 10.13031/aim.201800881).

Hodecker, B. E. R., Pita-Barbosa, A., de Barros, N. F., & Merchant, A. (2018). Water availability preceding long-term drought defines the tolerance of eucalyptus to water restriction. New Forests, 49(2), 173-195. doi:10.1007/s11056-017-9612-6

Holman, F. H., Riche, A. B., Michalski, A., Castle, M., Wooster, M. J., and Hawkesford, M. J. (2016). High throughput field phenotyping of wheat plant height and growth rate in field plot trials using UAV based remote sensing.Remote Sensing 8:1031. doi: 10.3390/rs8121031

Hunter, M. C., Smith, R. G., Schipanski, M. E., Atwood, L. W., Mortensen, D. A. (2017). Agriculture in 2050: Recalibrating Targets for Sustainable Intensification. BioScience, Volume 67, Issue 4, Pages 386–391.

Hunt Jr., E. R., Doraiswamy, P. C., McMurtrey, J. E., Daughtry, C. S. T., Perry, E. M., & Akhmedov, B. (2013). A visible band index for remote sensing leaf chlorophyll content at the canopy scale. International Journal of Applied Earth Observation and Geoinformation, 21, 103-112. doi: https://doi.org/10.1016/j.jag.2012.07.020

Hunt Jr., E. R., Daughtry, C. S. T., (2018). What good are unmanned aircraft systems for agricultural remote sensing and precision agriculture? . Volume 39, Issue 15-16 Pages 5345-5376.

Hu, P.C. et al. (2018) Estimation of plant height using a high throughput phenotyping platform based on unmanned aerial vehicle and self-calibration: example for sorghum breeding. Eur. J. Agron. 95, 24–32

Ikerd, J., as quoted by Richard Duesterhaus in "Sustainability's Promise". (1990) Journal of Soil and Water Conservation. 45(1): p.4. NAL Call # 56.8 J822.

Jackson, R. D. (1984). Remote Sensing of Vegetation Characteristics for Farm Management. SPIE Critical Reviews of Technology Series: Remote Sensing 475: 81–96. doi:10.1117/12.966243.

Joshua D. Rudd, Gary T. Roberson, & John J. Classen (2017) Application of satellite, unmanned aircraft system, and ground-based sensor data for precision agriculture: a review. 2017 ASABE Annual International Meeting DOI: https://doi.org/10.13031/aim.201700272 Paper Number: 1700272

Kang, L., Ji, C. Y., Kim, S. H., Ke, Q., Park, S. -., Kim, H. S., . . . Kwak, S. -. (2017). Suppression of the ß-carotene hydroxylase gene increases ß-carotene content and tolerance to abiotic stress in transgenic sweetpotato plants. Plant Physiology and Biochemistry, 117, 24-33. doi:10.1016/j.plaphy.2017.05.017

Khanal, S.; Fulton, J.P.; Hawkins, E.; Port, K. et al., "Remote Sensing in Precision Agriculture:Best Management Practices for Addressing Challenges with Imagery Quality" 2017.

Khanal, S., Fulton, J., Shearer, S. (2017). An overview of current and potential applications of thermal remote sensing in precision agriculture. Computers and Electronics in Agriculture 139 (2017) 22–32.

Khanal, S.; Fulton, J.P.; Hawkins, E.; Port, K. et al. (2017), "Remote Sensing in Precision Agriculture:Best Management Practices for Addressing Challenges with Imagery Quality" .

Kim, S. H., Ahn, Y. O., Ahn, M., Lee, H., & Kwak, S. (2012). Down-regulation of β- carotene hydroxylase increases β- carotene and total carotenoids enhancing salt stress tolerance in

transgenic cultured cells of sweetpotato. Phytochemistry, 74, 69-78. doi:10.1016/j.phytochem.2011.11.003

King CA, Purcell LC, Brye KR (2009) Differential wilting among soybean genotypes in response to water deficit. Crop Sci 49:290–298

Kingston, D.B., Beard, A.W., (2004) Real-time Attitude and Position Estimation for Small UAVs using Low-cost Sensors. In Proceedings of the AIAA 3rd Unmanned Unlimited Technical Conference on Workshop and Exhibit. Chicago, IL, USA.

Kyratzis, A.C. et al. (2017) Assessment of vegetation indices derived by UAV imagery for durum wheat phenotyping under a water limited and heat stressed Mediterranean environment. Front. Plant Sci. 8, 1114

Laliberte, A.S. Rango, A., (2011) Image Processing and Classification Procedures for Analysis of Sub-decimeter Imagery Acquired with an Unmanned Aircraft over Arid Rangelands. GI Science in Remote Sensing. 48, 4–23.

Lambert, J. et al. (2018) Evaluating the potential of unmanned aerial systems for mapping weeds at field scales: a case study with Alopecurus myosuroides. Weed Res. 58, 35–45

Lei Deng, Zhihui Mao, Xiaojuan Li, Zhuowei Hu, Fuzhou Duan, Yanan Yan 2018 UAV-based multispectral remote sensing for precision agriculture: A comparison between different cameras. ISPRS Journal of Photogrammetry and Remote Sensing 146 (2018) 124–136

Liu, T. et al. (2018) Estimates of rice lodging using indices derived from UAV visible and thermal infrared images. Agric. Forest Meteorol. 252, 144–154

Li W., Niu Z., Chen H. Y., Li D., Wu M. Q., Zhao W. (2016). Remote estimation of canopy height and aboveground biomass of maize using high-resolution stereo images from a low-cost unmanned aerial vehicle system. Ecol. Indic. 67, 637–648. 10.1016/j.ecolind.2016.03.036

López-Granados, F. et al. (2016a) Object-based early monitoring of a grass weed in a grass crop using high resolution UAV imagery. Agron. Sustain. Dev. 36, 67

López-Granados, F. et al. (2016b) Early season weed mapping in sunflower using UAV technology: variability of herbicide treat-ment maps against weed thresholds. Precis. Agric. 17, 183–199

Lucieer, A., Malenovský, Z., Veness, T., & Wallace, L. (2014). HyperUAS—Imaging spectroscopy from a multirotor unmanned aircraft system. Journal of Field Robotics, 31(4), 571-590.

Madec, S. et al. (2017) High-throughput phenotyping of plant height: comparing unmanned aerial vehicles and ground LiDAR estimates. Front. Plant Sci. 8, 2002

Maes, W.H. and Steppe, K. (2012) Estimating evapotranspira-tion and drought stress with ground-based thermal remote sensing in agriculture: a review. J. Exp. Bot. 63, 4671–4712 14.

Majidi, B., Bab-Hadiashar, A., (2005) Real time aerial natural image interpretation for autonomous ranger dronenavigation. In Proceedings of the Digital Imag Computing Techniques and Application (DICTA 2005), Cairns, QLD, Australia. pp. 448–453.

Mangus, D., A. Sharda, and N. Zhang. 2016. Development and Evaluation of Thermal Infrared Imaging System for High Spatial and Temporal Resolution Crop Water Stress Monitoring of Corn within a Greenhouse. Computers and Electronics in Agriculture. 121: 149-159. doi:10.1016/j.compag.2015.12.007.

Matese, A., Toscano, P., Di Gennaro, S., Genesio, L., Vaccari, F., Primicerio, J., . . . Gioli, B. (2015). Intercomparison of UAV, aircraft and satellite remote sensing platforms for precision viticulture. Remote Sensing, 7, 2971-2990.

Mesas-Carrascosa, F.J., Torres-Sánchez, J., Clavero-Rumbao, I., . . . , López-Granados, F., (2015). Assessing Optimal Flight Parameters for Generating Accurate Multispectral Orthomosaicks by UAV to Support Site-Specific Crop Management. Remote Sensing. 7, 12793-12814; doi:10.3390/rs71012793.

Mittal, A., Moorthy, A.K., Bovik, A.C., (2012). No-Reference Image Quality Assessment in the Spatial Domain. IEEE Transactions on Image Processing. Vol. 21, no. 12, 4695-4708.

Mittal, A., Soundararajan, R., Bovik, A.C., (2013). Making a “Completely Blind” Image Quality Analyzer. IEEE Signal Processing Letters. Vol. 20, no. 3, 209-212.

Möller, M., Alchanatis, V., Cohen, Y., Meron, M., Tsipris, J., Naor, A., . . . Cohen, S. (2007) Use of thermal and visible imagery for estimating crop water status of irrigated grapevine. Journal of Experimental Botany. 58, 827–838.

Moran, M. S., Inoue, Y., Barnes, E. M. (1997). Opportunities and Limitations for Image-Based Remote Sensing in Precision Crop Management. Remote Sensing of Environment. 61 (3): 319–346. doi:10.1016/S0034-4257(97)00045-X.

Mullan, D. J., and Reynolds, M. P. (2010). Quantifying genetic effects of ground cover on soil water evaporation using digital imaging. Funct. Plant Biol. 37,703–712. doi: 10.1071/Fp09277

Mulla, D., Khosla, R. (2016). Historical Evolution and Recent Advances in Precision Farming. In Soil-Specific Farming Precision Agriculture. CRC Press. doi:10.1201/b18759-2.Nijland, W. et al. (2014) Monitoring plant condition and phenol-ogy using infrared sensitive consumer grade digital cameras. Agric. Forest Meteorol. 184, 98–106

Ortega-Farías, S., Ortega-Salazar, S., Poblete, T., Kilic, A.; Allen, R.; Poblete-Echeverría, C., . . . Sepúlveda, D., (2016). Estimation of energy balance components over a drip-irrigated

olive orchard using thermal and multispectral cameras placed on a helicopter-based unmanned aerial vehicle (UAV). Remote Sensing. 8, 638.

Park, S.; Nolan, A.; Ryu, D.; Fuentes, S.; Hernandez, E.; Chung, H.; O'Connell, M. Estimation of crop water stress in a nectarine orchard using high-resolution imagery from unmanned aerial vehicle (UAV). In Proceedings of the 21st International Congress on Modelling and Simulation, Gold Coast, Australia, 29 November–4 December 2015; pp. 1413–1419.

Pinter, P. J., Hatfield, J. L., Schepers, J. S., Barnes, E. M., Moran, M. S., Daughtry, C. S. T., Upchurch, D. R, (2003). Remote Sensing for Crop Management. Photogrammetric Engineering & Remote Sensing. 69 (6): 647–664. doi:10.14358/PERS.69.6.647.

Rajan, N., and Maas, S. J. (2009). Mapping crop ground cover using airborne multispectral digital imagery. Precision Agric. 10, 304–318. doi: 10.1007/s11119-009-9116-2

Rembold, F. et al. (2013) Using low resolution satellite imagery for yield prediction and yield anomaly detection. Remote Sens. 5, 1704

Ribeiro-Gomes, K., Hernández-López, D., Ortega, J. F., Ballesteros, R., Poblete T., Moreno, M. A., (2017). Uncooled Thermal Camera Calibration and Optimization of the Photogrammetry Process for UAV Applications in Agriculture. Sensors. 17, 2173; doi:10.3390/s17102173.

Robert, P. C. (1982). Evaluation of Some Remote Sensing Techniques for Soil and Crop Management. Ph.D. Dissertation. Minneapolis: University of Minnesota.

Rockström, J. et al. (2017)Sustainable intensification ofagriculture for human prosperity and global sustainability. Ambio 46, 4–17 12.

Rud, R.; Cohen, Y.; Alchanatis, V.; Levi, A.; Brikman, R.; Shenderey, C., . . . Rosen, C. (2014). Crop water stress index derived from multi-year ground and aerial thermal images as an indicator of potato water status. Precision Agriculture. 15, 273–289.

Sankaran, S., Khot, L. R., and Carter, A. H. (2015). Field-based crop phenotyping: multispectral aerial imaging for evaluation of winter wheat emergence and spring stand. Comp. Electron. Agric. 118, 372–379. doi: 10.1016/j.compag.2015.09.001

Sankaran, S., Mishra, A., Ehsani, R., & Davis, C. (2010). A review of advanced techniques for detecting plant diseases. Computers and Electronics in Agriculture, 72(1), 1-13. doi:10.1016/j.compag.2010.02.007

Santesteban, L.G., Di Gennaro, S.F., Herrero-Langreo, A., Miranda, C., Royo, J.B., Matese, A. (2017) High-resolution UAV-based thermal imaging to estimate the instantaneous and seasonal variability of plant water status within a vineyard. Agricultural Water Management. 183, 49–59.

Senthilnath, J., Kandukuri, M., Dokania, A., Ramesh, K.N., (2017). Application of UAV imaging platform for vegetation analysis based on spectral-spatial methods. Computers & Electronics in Agriculture. 140, 8–24.

Schirrmann, M. et al. (2016) Monitoring agronomic parameters of winter wheat crops with low-cost UAV imagery. Remote Sens. 8, 706

Shi, Y., Murray, S. C., Rooney, W. L., Valasek, J., Olsenholler, J., Pugh, N. A., . . . Thomasson, J. A. (2016). Corn and sorghum phenotyping using a fixed-wing UAV-based remote sensing system. Autonomous Air and Ground Sensing Systems for Agricultural Optimization and Phenotyping,

Sugiura R., Noguchi N., Ishii K. (2005). Remote-sensing technology for vegetation monitoring using an unmanned helicopter. Biosys. Eng. 90, 369–379. 10.1016/j.biosystemseng.2004.12.011

Swain, K. C., Jayasuriya, H. P., & Salokhe, V. M. (2007). Suitability of low- altitude remote sensing images for estimating nitrogen treatment variations in rice cropping for precision agriculture adoption. Journal of Applied Remote Sensing, 1(1) doi:10.1117/1.2824287

Tamouridou, A.A. et al. (2017) Application of multilayer percep-tron with automatic relevance determination on weed mapping using UAV multispectral imagery. Sensors 17, 2307

Tamouridou, A. A., Alexandridis, T. K., Pantazi, X. E., Lagopodi, A. L., Kashefi, J., and Moshou, D. (2017). Evaluation of UAV imagery for mapping Silybum marianum weed patches. Int. J. Remote Sensing 38, 2246–2259. doi: 10.1080/01431161.2016.1252475.

Tilling, A. K., O'Leary, G. J., Ferwerda, J. G., Jones, S. D., Fitzgerald, G. J., Rodriguez, D., & Belford, R. (2007). Remote sensing of nitrogen and water stress in wheat. Field Crops Research, 104(1–3), 77-85. doi:https://doi.org/10.1016/j.fcr.2007.03.023

Wang, J.-J. et al. (2018) Unsupervised discrimination between lodged and non-lodged winter wheat: a case study using a low- cost unmanned aerial vehicle. Int. J.Remote Sens. 39, 2079–2088

Watanabe, K. et al. (2017) High-throughput phenotyping of sor- ghum plant height using an unmanned aerial vehicle and its appli- cation to genomic prediction modeling. Front. Plant Sci. 8, 421

Weiss, M., and Baret, F. (2017). Using 3D point clouds derived from UAV RGB imagery to describe vineyard 3D Macro- structure. Remote Sensing 9:17. doi: 10.3390/rs9020111

Wouter H. Maes, and Kathy Steppe. 2019. Perspectives for remote sensing with unmanned aerial vehicles in precision agriculture. Trends in Plant Science, February 2019, Vol. 24, No. 2, Pg. 152-164.

Yang, C., Everitt, J. H., & Fernandez, C. J. (2010). Comparison of airborne multispectral and hyperspectral imagery for mapping cotton root rot doi:http://dx.doi.org/10.1016/j.biosystemseng.2010.07.011

Yang, G.J. et al. (2017) Unmanned aerial vehicle remote sensing for field-based crop phenotyping: current status and perspec-tives. Front. Plant Sci. 8, 1111

Yang, M.-D. et al. (2017) Spatial and spectral hybrid image classification for rice lodging assessment through UAV imagery. Remote Sens. 9, 583

Yu, K., Kirchgessner, N., Grieder, C., Walter, A., and Hund, A. (2017). An image analysis pipeline for automated classification of imaging light conditions and for quantification of wheat canopy cover time series in field phenotyping. Plant Methods 13:15. doi: 10.1186/s13007-017-0168-4

Yue, J.B. et al. (2017) Estimation of winter wheat above-ground biomass using unmanned aerial vehicle-based snapshot hyper-spectral sensor and crop height improved models. Remote Sens. 9, 708

Zaman-Allah, M., Vergara, O., Araus, J. L., Tarekegne, A., Magorokosho, C., Zarco-Tejada, P. J., et al. (2015). Unmanned aerial platform-based multispectral imaging for field phenotyping of maize. Plant Methods 11:10.doi: 10.1186/s13007-015-0078-2

Zarco-Tejada, P. J., Berjón, A., López-Lozano, R., Miller, J. R., Martín, P., Cachorro, V., . . ., De Frutos, A. (2005). Assessing vineyard condition with hyperspectral indices: Leaf and canopy reflectance simulation in a row-structured discontinuous canopy. Remote Sensing of Environment. 99, 271–287.

Zarco-Tejada, P.J. et al. (2013) A PRI-based water stress index combining structural and chlorophyll effects: assessment using diurnal narrow-band airborne imagery and the CWSI thermal index. Remote Sens. Environ. 138, 38–50

Zhang, C., Kovacs, J.M., (2012). The application of small unmanned aerial systems for precision agriculture: A review. Precision Agriculture. 13, 693–712.

Zhao, D., Huang, L., Li, J., Qi, J., (2007). A comparative analysis of broadband and narrowband derived vegetation indices in predicting LAI and CCD of a cotton canopy. Isprs J. Photogramm. Remote Sens. 62 (1), 25–33.

Zhou, X. et al. (2017) Predicting grain yield in rice using multi-temporal vegetation indices from UAV-based multispectral and digital imagery. ISPRS J. Photogramm. Remote Sens. 130, 246–255

Zarco-Tejada, P. J., Berjón, A., López-Lozano, R., Miller, J. R., Martín, P., Cachorro, V., . . ., De Frutos, A. (2005). Assessing vineyard condition with hyperspectral indices: Leaf and canopy reflectance simulation in a row-structured discontinuous canopy. Remote Sensing of Environment. 99, 271–287.